We thank the reviewers for their constructive feedback and suggested corrections. Below we have addressed each individual comment from reviewers #1 and #2 (reviewer comments are shown in italics; our responses to the reviewers' comments are shown in bold). In light of the reviewers' comments, our revised manuscript now includes (a) an analysis on the role of CH4 retrieval systematic biases, and (b) a more robust quantification of the CH_4 flux requirements. All manuscript changes are highlighted as 'tracked changes' in the revised manuscript (the bracketed line numbers denote the corresponding line numbers in the revised manuscript). We believe that the following revisions have substantially improved the overall quality of our manuscript.

Anonymous Referee #1

The paper by Bloom et al. investigates the required performance parameters of satellite missions aimed at gaining quantitative insight into the biogeochemical processes driving methane wetland emission in the Amazon region. To this end, the authors first examine the variability (in space, time, magnitude) of the carbon cycle and hydrological processes that control CH4 emissions. Then, they use observing system experiments to derive mission requirements (spatial and temporal resolution; precision) that would allow for disentangling the processes under natural variability. The study covers satellite concepts in low-earth-orbit (LEO) as well as in geostationary orbit (GEO).

The applied methodology is most interesting since it outlines an approach how to quantitatively derive mission requirements based on the actual variability of the targeted process parameters. I would tend to criticize the study as being too simplistic in one or the other way outlined below. But certainly, the paper is well written, methods are robust and rigorous, and thus, it is suitable for publication in ACP after considering my questions/comments below.

Questions/comments:

(1.1) (1) A shortcoming of the study is the assumption of purely random error sources implying that measurement uncertainty improves with the square root of the number of binned soundings. This assumption results in maps such as Figure 4 where the measurement precision of GEO soundings binned on 300×300 km2 is in the range of 0.1 ppb (given 1800 ppb background) which is a clearly unrealistic assumption for the overall measurement error. Experience with the current generation of passive greenhouse gas sounders such as GOSAT and OCO-2 tells that, at aggregated scales, random errors are dwarfed by systematic errors which typically exceed 0.1 ppb by far. Systematic errors are hard to address and, indeed, the manuscript concedes the neglect of systematic errors but a major caveat should be issued when discussing the achievable flux precisions.

We have now amended our analysis with an explicit simulation of CH_4 residual bias errors. We describe the incorporation of a residual CH_4 bias structure at the end of section 2.3 of the revised manuscript (P14 L3-17). We now show that the relative advantage of a GEO mission – in comparison to a LEO mission – decreases with increasing CH_4 bias (Figure 7). We have revised the results and discussion section (P15 L17-24), and the abstract (P1 L25 – P2 L3) to reflect this.

(1.2) (2) The manuscript restricts the advantage of a GEO sounder to massively enhanced data density. Wouldn't it make sense to actually exploit the quasi-contiguous temporal sampling of a GEO sounder? A GEO sounder would allow for resolving variability due to source and transport patterns on the time scale of hours. Running an inverse model with monthly flux resolution (and probably imposed sub-monthly variability) might simply discard some of the available process information.

We agree that additional constraints may be achievable under certain process scenarios; for example, emissions from spatially concentrated wetland CH_4 sources (e.g. across the main stem of the Amazon river) could potentially be constrained based on higher resolution CH_4 concentration gradients, and fluxes can be estimated using alternative approaches. Conversely, monthly CH_4 inversions are more suitable for spatially and temporally diffuse CH_4 emission process scenarios. We now discuss the additional potential advantages of GEO OS in the revised manuscript (P17 L13-16).

Technical comments:

(1.3) P5,L16: Focusing the study on March reduces data amount and related logistics but it neglects seasonal variability. Is there any indication that March is a benign or malign case? For example: is the CH_4 flux precision requirement of 3 mg CH4/m2/day valid for all seasons?

We have now included a more robust quantification of the CH_4 precision requirement: for a given resolution requirement, we derive a year-round precision requirement (now 10mg m^{-2} day^{-1}) as the CH_4 precision needed to statistically distinguish between wetland CH_4 process hypotheses with a 95% confidence. The precision requirement and its derivation are described in P7 L4-6, P8 L15 –P9 L6 and Appendix B. The results of our precision requirement analysis are shown in Figure 4.

In the reviewer's words, March 2007 is a "malign case": we now state that "the atmospheric CH_4 OS requirement as the ability to meet the CH_4 flux resolution and precision requirements during the cloudiest time of year" (P5 L19-20). We also clarify March 2007 is the cloudiest month in the Jan – Apr 2007 season (84% cloud cover) and it is considerably higher than the subsequent dry season (46% - 56% cloud cover) in P5 L22-24.

(1.4) P5,L16: MODIS cannot provide information on diurnal variability in cloud cover. Would you expect a significant effect e.g. for choosing an optimal LEO overpass or for optimizing GEO revisits?

We agree with the reviewer that diurnal variability may amount to a key component of assessing and optimizing GEO and LEO missions. Based on ERA-interim cloud-cover re-analyses, we show that the annual mean diurnal coefficient of variation of cloud-free Amazon basin spans 7% - 80% (median = 29%). Given the non-linear relationship between data yield and 1km x 1km cloud-free domain shown in Figure B1, we highlight that choice of diurnal variability could have a substantial influence on LEO and GEO data yield. We now make these points in the discussion section of our revised manuscript (P16 L22 – P17 L2).

(1.5) P7,L8: Looking at the correlation matrix (Figure A1), there is substantial correlation among (C1, C2, C4) and (H1,H2) on spatial scales down to 100 km which means that they would be hard to distinguish by an observing system. So, actually, the requirement L≤300 km only allows for discriminating carbon and hydrological controls but not for discriminating the type of carbon (except for C3 vs (C1,C2,C4)) or the type hydrological process (except for H3 vs (H1,H2)). Is that correct? Probably, this should be discussed in more detail.

We have now removed this figure (formerly "Figure A1") from the revised manuscript, since our precision derivation approach implicitly accounts for both spatial and temporal correlations (see response to 1.3 and Figure 4).

(1.6) P9,L1: It would be appropriate to cite an original TROPOMI paper at least once (instead of Wecht et al., 2014, repeatedly): P. Veefkind, I. Aben, K. McMullan, H. Förster, J. de Vries, G. Otter, J. Claas, H.J. Eskes, J.F. de Haan, Q. Kleipool, M. van Weele, O. Hasekamp, R. Hoogeveen, J. Landgraf, R. Snel, P. Tol, P. Ingmann, R. Voors, B. Kruizinga, R. Vink, H. Visser, P.F. Levelt, TROPOMI on the ESA Sentinel-5 Precursor: A GMES mission for global observations of the atmospheric composition for climate, air quality and ozone layer applications, Remote Sensing of Environment, Volume 120, 15 May 2012, Pages 70-83, ISSN 0034-4257, http://dx.doi.org/10.1016/j.rse.2011.09.027.

We now cite the Veefkind et al., (2012) paper as a reference for the TROPOMI mission in P4 L23 and P15 L14.

(1.7) P10,L9: "March and September 2007". The rest of the paper is restricted to March. So, I guess, September needs to be removed.

We have now removed "September".

(1.8) Equation (2): The multiplication of the vectors N and O is not a scalar product but an element-wise multiplication, right? Probably, this needs to be stated somewhere.

We now use an appropriate symbol and explicitly state this in P12 L21.

(1.9) P11,L7: Is the unperturbed CH4 flux assumed constant (12 mg/m2/day) throughout the domain?

In response to the second reviewer's comments (see responses to 2.2 and 2.9) we now report flux uncertainties in mg m^{-2} day^{-1}, and we have revised equation 5 accordingly. Since the explicit definition of f{L,0} is now redundant, it has been removed from the revised manuscript.

(1.10) P11,L17: Figure A2 -> Figure C1

We now correctly reference figure "D1" (previously figure C1) in P13 L11 of the revised manuscript.

(1.11) P11,L11: A further advantage of GEO is several revisits per day.

We now clearly state this in P14 L24 – P15 L2 of the revised manuscript

(1.12) Appendices: It would be useful to have a meaningful title for the appendices (instead of only Appenix A, B, C).

We have now added descriptive titles to Appendices A-D.

(1.13) Equation C1: What is the inverse of a vector, f'−1?

We have now added a sentence to better clarify that f' is an N × N array, comprised of N flux vectors (P21 L16-18).

(1.14) P16,L22: Figure A1 -> Figure A2.

Figure reference now corrected

Anonymous Referee #2

This study presents an OSSE for different hypothetical LEO and GEO satellite instruments. The focus is on the requirements on these observing systems for obtaining process-relevant information on wetland emissions in the Amazon region. As explained below some assumptions are made, which are not well justified but have a potentially large influence on the conclusions. These will have to be dealt with in a satisfactory manner to make this paper suitable for publication in ACP.

GENERAL COMMENTS

(2.1) Autocorrelation scales have been derived for several parameters to motivate the choice of spatial scale that the measurements should be able to resolve in order for the OS to help us gain process understanding. It is presented as a novel approach that could be applied to other related problems. Although I appreciate the attempt to derive such scales (which indeed addresses an important question), I do not agree that the presented method solves this problem. The reason is that the results presented in figure 3 depend on the scale of the data sets that are used. What is shown is the autocorrelation of parameters that are averaged on a scale of 0.5x0.5 degree. If the resolution of the datasets were much higher, then other more local processes would contribute to variability shortening the overall auto-correlation scale. Indeed it is questionable whether the methane emission from a local pond really correlates with one that is 100 km away. What is the motivation to use datasets at 0.5x0.5 degree? If the processes themselves motivate this choice then this should be explained. In absence of such a motivation it is a probably more a practical choice. I have no problem with this choice as long as its limitation is made clear, and that it requires reconsideration for any other application.

We agree with the reviewer that our assessment of carbon and hydrological process variable correlation scales requires reconsideration for any subsequent application. We now clarify that the auto-correlation scales are specific to the Amazon river basin; we also highlight the limitation of our auto-correlation approach, and we clarify that finer-scale analyses may require higher resolution datasets to quantify GHG measurement requirements (P17 L4 – 5 and P17 L8-11).

We also agree with the reviewer that finer-scale variability from higher-resolution datasets could potentially contribute to alternative assessments of auto-correlation scales. However, in our derivation of Moran's I at each *L*, we aggregate our data at an L × L resolution (see Appendix A), and therefore fine-scale variability is averaged out (regardless of the native resolution of the dataset).

(2.2) If it is considered important that the inversion resolves the autocorrelation scale then it is not sufficient to evaluate the posterior uncertainty at that scale. This is because the off-diagonals of the posterior covariance matrix might indicate that neighboring fluxes are not independently determined. In this study, however, the performance criterion only considers values on the diagonal. In addition, the choice of 25% confuses monthly and annual fluxes. The requirement is on monthly fluxes, but it is derived from an estimate of Melack et al on the annual time scale.

We agree with the reviewer that using a "%" precision is misleading. We now present flux precision in flux units (mg CH_4 m^{-2} day^{-1}) throughout the manuscript and in Figures (6-8). The units are now consistent with our

revised precision requirement (10mg/m^2/day; see response to reviewer comment 1.3).

We agree with the reviewer that "off-diagonal" error correlations in retrieved fluxes would likely indicate that neighbouring fluxes are not independently determined. However, as long as all diagonal terms meet the precision requirement (10mg/m^2/day), the OS can resolve underlying spatial flux patterns at the required precision (regardless of posterior error covariance).

(2.3) It is unclear why a special effort is made to derive requirements on horizontal resolution looking at the drivers of processes, whereas this is not done for the requirements on flux precision and temporal resolution. Since the inversion solves for net fluxes it remains unclear anyway if these requirements really allow us to constrain specific processes. Wouldn't it have been more logical to vary process model parameters to determine what is needed to resolve them? You might wonder whether it is even realistic to constrain processes only by measuring XCH4 using a single instrument. Atmospheric measurements are useful for constraining regional emission budgets, which - in combination with other information - can be used to derive improved process under- standing. The OSSE approach that is taken disqualifies instruments that provide useful constraints on larger scales as part of a multi-component global monitoring system.

We now include a quantification of the CH_4 flux precision requirements for distinguishing between both spatial and temporal CH_4 emission hypotheses (see response to reviewer comment 1.3). We have also now included a lagged Pearson's correlation analysis to determine the temporal process control correlation lengths (P8 L5-11).

We agree with the reviewer that varying process parameters in a model is potentially a useful approach for quantifying the OS needed to improve process understanding. However, due to the scarcity of top-down constraints and in-situ measurements in tropical wetland environments (P6 L23 – P7 L1), little is known about whether current models are able to capture the first-order spatial and temporal variability of wetlands. We have expanded our discussion in P17 L20 - P18 L9 to clearly state that model approaches can be used – albeit with due caution – to define CH_4 OS measurement requirements of the revised manuscript.

We also highlight the need to investigate the added advantages of a multi-component global monitoring system in P17 L16-18 of the revised manuscript.

(2.4) This OSSE is extremely (and unrealistically I would say) optimistic about the uncertainty reduction that can be achieved by averaging large numbers of data. It is mentioned that the 'cumulative' uncertainty of GEO OS may be as low as 0.02 ppb. It is probably a main reason why the GEO measurement concept performs so well in this study. In reality, however, systematic uncertainties will kick in at much reduced

precisions preventing any further improvements upon averaging. Some attempt should be made to assess the sensitivity of the conclusion that improved process-understanding calls for the GEO approach, to the presence of systematic errors in the data.

We agree with the reviewer that systematic biases are a limiting factor in the potential performance of a GEO approach. We have now included a residual CH_4 bias analysis to address this comment (see response to comment 1.1).

(2.5) Further effort is needed to quantify the impact of errors due to the simplified treatment of atmospheric transport. In general, surface fluxes are proportional to spatio-temporal concentration gradients in the atmosphere. Looking at figure C1 it becomes clear that the east-west gradient in WRF is substantially stronger than in LPDM. It has probably to do with the north- and southward transport along the Andes in WRF, which is missing in LPDM. The impact of this should be quantified.

We agree with the reviewer that the LPDM approach underestimates the east-west gradient (see response to 2.18), and we now highlight that the LPDM provides a conservative estimate on the observable CH_4 gradients across the region (P16 L12-14). To quantify the potential bias stemming from underestimated CH_4 gradient across the Amazon domain, we conduct a sensitivity test on the GEO and LEO median flux precision retrievals, where the LPDM-derived transport operator is multiplied by 1.5. We find that this leads to an inversely proportional (~33%) reduction in the GEO and LEO flux precision (we report this in lines P16 L14-16 of the revised manuscript).

(2.6) It should be made clearer why the analysis is limited to the month of March. Many things are different in other months (atmospheric dynamics, cloud cover, CH4 fluxes, etc.). March doesn't sound like a particularly good choice as average, or representative month.

We now define our OS requirements as the ability to resolve monthly CH_4 fluxes at the required resolution and precision during the cloudiest part of the 2007 wet season (see response to comment 1.3). We also highlight that March is the cloudiest month in the 2007 wet season (P5 L23-25). Finally, we highlight the need to investigate the role seasonal transport variability (amongst other factors) on GEO and LEO CH_4 flux retrievals (P16 L18-20).

SPECIFIC COMMENTS

(2.7)Page 7, line 14: 'Throughout ... CH4 emissions" I don't see why the fact that 25% is in between the dynamic ranges of monthly GPP and inundation variability would make it suitable for separating their influences. Apart from this, what justifies the assumed linearity between these drivers and methane emissions?

We have now addressed this concern with a more robust derivation of CH_4 flux requirements (see response to comment 1.3).

(2.8)Page 9, line 11: 'i.e. all accepted ... 100% cloud-free' According to Appendix B, MODIS data that is probably cloud-free are considered as fully cloud-free. These two statements do not fit together.

We have grouped "probably cloud free" and "cloud free" flags together, and "probably cloudy" and "cloudy" flags together. We have clarified this in P11 L8-10 in the revised manuscript, and we have added a sentence in Appendix C to clarify our assumptions (P21 L4-6).

(2.9)Page 11, equation 3: Why is c{L,0} calculated? In the end all that matters is the spread in 'c' due to the random perturbation and how it maps on 'f' using 'A'. The uncertainty in 'f' does not depend on the mean of 'c'.

We agree with the reviewer's statement, since our derivation of *f* (equation 5) is independent of c{L,0}. For the sake of simplicity, we now set all c{L,0} values to zero: we clarify this in P13 L15-16 of the revised manuscript.

(2.10)Page 13, line 21: 'If Amazon CH4 fluxes .... likely be lower' This depends on the distribution of cloud cover. The wettest regions will likely be measured the least frequent. This calls for further motivation of why uniform emissions have been assumed.

In the revised manuscript, we now clearly define our OS requirement as the ability to statistically distinguish between biogeochemical process hypotheses based on cloud cover statistics during the cloudiest time of the 2007 wet season (P5 L23-25, and see response to comment 1.3).

(2.11)Page 15, line 7: Why is the purpose of the parentheses here? Please clarify further at what p-level the autocorrelations are required to be significant, and how this is determined. For example in the following sentence if is not clear what r_i refers to. Please revise the description to explain more clearly what was done.

We have now revised this sentence to better convey our derivation of the Moran's I p-value (P19 L6-8).

(2.12) Figure 1: What are the different lines in the inset figure?

The green lines denote the average WETCHIMP model Amazon basin monthly CH_4 emissions. We have revised the figure caption to clarify this.

(2.13)Figure 4: Why do you call this 'cumulative precision'? Isn't it rather the precision of a 300x300km2 average?

We now explicitly define CH_4 "cumulative precision" in P10 L10-11 of the revised manuscript. For the sake of clarity, we also define CH_4 "cumulative precision" in the figure caption (now Figure 5).

(2.14)Figure 5: Why isn't cloud filtering affecting the number of data, comparing GEO, GEO- Z1, GEO-Z2?

Observations per unit area include all attempted measurements (both cloud and cloud-free measurements). We have revised the figure caption (now Figure 6) to reflect this.

(2.15)Figure B1: I assume that both panels represent March 2007. If so, then this should be made clear.

Figure caption updated

(2.16) Figure C1: Do these values represent the total column? If so, then mention this.

Figure caption updated

(2.17)Appendix B, line 18: f(omega,i) is not used in equation 1. Where do the 30x30km2 areas come from?

We now correctly use 'phi' (as opposed to 'f') in referencing the fraction of cloud-free observations in equation 1. We have also corrected '30x30km' to 'L × L'. (P21 L8-9)

(2.18) Appendix C, line 17: The mean in CH4 is not the relevant quantity to compare LPDM and WRF (it is the gradient in the wind direction that matters).

We now also report the LPDM-approach and WRF gradients across the domain in Appendix D (P23 L11-13; 13.14ppb and 17.24ppb respectively); we calculate the gradients as the CH_4 difference between the North-East and South-West sub-regions of Amazon basin domain. We have also updated Figure D1 to mark the delineation between the "North-East" and "South-West" regions.

Additional changes

We have rectified a minor bug in our Moran's I code. We have updated the results and Figure 3 accordingly.

For consistency with the new precision requirement derivation, we have changed our spatial CH_4 requirement from "300km" to "~333km".

We have updated Figure 8 to include bias simulations and the precision and resolution requirements.

We have removed the first paragraph of Appendix A, as the text was redundant.

What are the greenhouse gas observing system requirements for reducing fundamental biogeochemical process uncertainty? Amazon wetland CH_4 emissions as a case study.

A. Anthony Bloom[1], Thomas Lauvaux[1,2], John Worden[1], Vineet Yadav[1], Riley Duren[1], Stanley Sander[1], David Schimel[1].

[1]Jet Propulsion Laboratory, California Institute of Technology, Pasadena, CA

[2] Department of Meteorology, The Pennsylvania State University, University Park, PA

Correspondence to: A. Anthony Bloom (abloom@jpl.nasa.gov)

Abstract. Understanding the processes controlling terrestrial carbon fluxes is one of the grand challenges of climate science. Carbon cycle process controls are readily studied at local scales, but integrating local knowledge across extremely heterogeneous biota, landforms and climate space has proven to be extraordinarily challenging. Consequently, top-down or integral flux constraints at process-relevant scales are essential to reducing process uncertainty. Future satellite-based estimates of greenhouse gas fluxes – such as CO_2 and CH_4 – could potentially provide the constraints needed to resolve biogeochemical process controls at the required scales. Our analysis is focused on Amazon wetland CH_4 emissions, which amount to a scientifically crucial and methodologically challenging case study. We quantitatively derive the observing system requirements for testing wetland CH_4 emission hypotheses at a process-relevant scale. To distinguish between hypothesized hydrological and carbon controls on Amazon wetland CH_4 production, a satellite mission will need to resolve monthly CH_4 fluxes at a ~333km resolution and with a ≤10 mg CH_4 m^{-2} d^{-1} flux precision. We simulate a range of low-earth orbit (LEO) and geostationary orbit (GEO) CH_4 observing system configurations to evaluate the ability of these approaches to meet the CH_4 flux requirements. Conventional LEO and GEO missions resolve monthly ~333km Amazon wetland fluxes at a 17.0 mg CH_4 m^{-2} d^{-1} and 2.7 mg CH_4 m^{-2} d^{-1} median uncertainty level. Improving LEO CH_4 measurement precision by $\sqrt{2}$ would only reduce the median CH_4 flux uncertainty to 11.9 mg CH_4 m^{-2} d^{-1}. A GEO mission with targeted observing capability could resolve fluxes at a 2.0 – 2.4 mg CH_4 m^{-2} d^{-1} median precision by increasing the observation density in high cloud-cover regions at the expense of other parts of the domain. We find that residual CH_4 concentration biases can

potentially reduce the ~5-fold flux CH_4 precision advantage of a GEO mission to a ~2-fold advantage (relative to a LEO mission). For residual CH_4 bias correlation lengths of 100km, the GEO can nonetheless meet the ≤10 mg CH_4 m^{-2} d^{-1} requirements for systematic biases ≤10ppb. Our study demonstrates that process-driven greenhouse gas observing system simulations can enhance conventional uncertainty reduction assessments by quantifying the OS characteristics required for testing biogeochemical process hypotheses.

1. Introduction

Quantitative knowledge of biogeochemical processes regulating global carbon-climate feedbacks remains highly uncertain (Friedlingstein et al., 2013). Quantifying the sensitivity of biogeochemistry to climate variables directly from observations of atmospheric concentrations has long been a goal of researchers (Bacastow et al., 1980; Vukicevic et al, 1997; Gurney et al., 2008). Estimating the climate sensitivity of carbon fluxes is complicated by both the spatial scale and structure of climate anomalies and the variations of factors affecting ecosystem responses: soils, vegetation, land use and natural disturbance (King et al., 2015). Current ground-based and even space-based carbon cycle observing systems produce flux estimates at continental or even zonal resolution, limiting direct estimation of relationships between climate forcing, ecosystem properties and carbon fluxes (Huntzinger et al., 2012, Peylin et al., 2013). The uncertainty of carbon fluxes at continental and finer scales is high, and different systems for flux estimation often produce strikingly different spatial patterns (Schimel et al 2015a; Bloom et al., 2016). Because of the high uncertainty in the spatial regionalization of fluxes, some of the most compelling studies of carbon and climate have eliminated the spatial information and instead have used correlative approaches to identify the regions likely to be responsible for observed global concentration anomalies (Braswell et al., 1997; Cox et al., 2013; Chen et al., 2015; Franklin et al., 2016).

The expansion of surface and aircraft observing networks has increased our understanding of the carbon cycle, and is essential for precise quantification of trace gas concentrations (Andrews et al., 2014, Sweeney et al., 2015; Wilson et al., 2016). Surface networks are intrinsically limited in their density, by cost, access to remote terrestrial and marine environments, environmental conditions and other logistical constraints (Schimel et al., 2015b). The first-generation trace

gas observing satellites were designed to make global-scale measurements of concentrations with unprecedented frequency and accuracy, but were not designed to test specific hypotheses about biogeochemical processes. The successes of GOSAT (Yokota et al., 2009) and OCO-2 (Crisp et al., 2004) open the door to designing a next generation of spaceborne greenhouse gas measurements to test specific hypotheses about the terrestrial biosphere or the oceans. In this paper, we report an observing system design exercise aimed at identifying the observing system needed to increase understanding of a long-standing uncertainty in the global carbon budget, specifically the role of tropical wetlands in the global CH_4 budget (Mitsch et al., 2010; Bloom et al., 2010; Melton et al., 2013). While we focus this analysis on CH_4, we note that the models and methodology are equally applicable to other gases (such as CO_2), and other regions or mechanisms.

Wetland CH_4 emissions

Biogenic methane (CH_4) emission processes are one of the principal components of global carbon-climate interactions; CH_4 is a potent greenhouse gas (Myhre et al., 2013) and wetlands account for roughly 20-40% of the global CH_4 source (Kirschke et al., 2013). The processes controlling the magnitude and temporal evolution of CH_4 outgassing from wetland environments remain largely un-quantified on continental scales. As a result, global scale wetland CH_4 emissions (Melton et al., 2013) and their role in the inter-annual growth of atmospheric CH_4 remain highly uncertain.

Global wetland CH_4 emissions largely depend on soil inundation, temperature and substrate carbon availability. The major sources of wetland CH_4 emissions include boreal North America, boreal Eurasia, the Indonesian archipelago, the Congo and Amazon river basins (Figure 1, map) which are all characterized by high soil carbon content (Hiederer and Köchy, 2011) and substantial seasonal or year-round inundation extent (Prigent et al., 2012). By and large, Amazon wetland CH_4 emissions dominate both the magnitude and uncertainty of global wetland CH_4 emissions (Melton et al., 2013). Estimates of Amazon wetland CH_4 emissions range between 20 – 60 Tg CH_4 yr^{-1} (Fung et al., 1991; Riley et al., 2011; Bloom et al., 2012; Melack et al., 2004), roughly equivalent to 10 – 30% of the global wetland CH_4 source. Major uncertainties are also associated with the spatial and temporal variability of CH_4 emissions (Figure 1). Uncertainties in tropical wetland CH_4 emission estimates

largely stem from a lack of quantitative knowledge of process controls on wetland CH_4 emissions, and a lack of data constraints on the drivers of wetland emissions. In terms of processes, a range of factors including soil pH, wetland vegetation cover, wetland depth, salinity and air-water gas exchange dynamics, likely impose fundamental controls on the rate of wetland CH_4 emissions. On a continental scale, spatially-explicit knowledge of carbon cycling and inundation remain highly uncertain in the wet tropics, primarily due to a sparse in-situ measurement network, high cloud cover and biomass density

Top-down CH_4 flux estimates

Top-down constraints on CH_4 fluxes – from atmospheric CH_4 observations – are key to retrieving quantitative information on continental-scale CH_4 biogeochemistry (Bousquet et al., 2011; Pison et al., 2013; Basso et al., 2016; Wilson et al., 2016). Low-earth orbit satellite missions, including SCIAMACHY, IASI, TES, and GOSAT have surveyed global CH_4 concentrations for over a decade (Frankenberg et al., 2008; Crevoisier et al., 2009; Butz et al., 2011; Worden et al., 2012). In particular, column CH_4 retrievals from SCIAMACHY have proven sensitive to wetland and other CH_4 emissions (Bloom et al., 2010; Bergamaschi et al., 2013). However, cloud cover is a major inhibiting factor when measuring atmospheric greenhouse gas concentrations within the proximity of tropical wetland regions. In particular, densely vegetated seasonally inundated areas of the Amazon and Congo river basins can experience more than 95% monthly mean cloud cover. With fewer cloud-free observations of lower tropospheric CH_4 concentrations, atmospheric inversion estimates of wetland CH_4 emissions remain exceedingly difficult, especially in the absence of well-characterized prior information on the magnitude, location and timing of emissions.

Atmospheric inverse estimates of CH_4 emissions are expected to improve with tropospheric CH_4 measurements from the upcoming ESA TROPOMI mission (Butz et al., 2012; Veefkind et al., 2012). Furthermore, geostationary missions (such as GEOCAPE) will potentially provide the measurements needed to substantially improve CH_4 emission estimates (Wecht et al., 2014; Bousserez et al., 2015). Ultimately, the precision and sampling configuration of atmospheric CH_4 observations

both determine the observing system (OS) capability of retrieving surface CH_4 fluxes. It is currently unclear whether future CH_4 measurements will be sufficient to resolve key CH_4 fluxes – such as the Amazon basin wetlands – at a process-relevant resolution.

In this study we characterize the satellite observations required to quantify the biogeochemical process controls on Amazon wetland CH_4 emissions. Specifically, we identify and characterize the Amazon CH_4 emission processes (section 2.1), define the process-relevant CH_4 flux resolution and precision required to statistically distinguish between hypothesized wetland CH_4 emission scenario based on several hydrological and carbon datasets (section 2.2), we simulate atmospheric measurements throughout the Amazon basin for a range of low-earth orbit and geo-stationary orbit satellite OS, and we derive the corresponding CH_4 flux uncertainty using an idealized atmospheric inversion (section 2.3). Based on our results, we establish the OS requirements and discuss the potential of future OS to resolve Amazon wetland CH_4 emission processes (section 3). We conclude our paper in section 4.

2. Methods

We construct an Observing System Simulation Experiment (OSSE) dedicated to characterizing the spaceborne OS needed to resolve the processes controlling wetland CH_4 fluxes from Amazon basin (Figure 2). Our OSSE involves the following 3 steps: we (1) characterize the variability of wetland CH_4 process controls; (2) define CH_4 flux resolution and precision requirements; and (3) derive the atmospheric CH_4 concentration OS requirements. We define the atmospheric CH_4 OS requirement as the ability to meet the CH_4 flux resolution and precision requirements during the cloudiest time of year. We focus our analysis on March 2007: all temporally-resolved carbon and hydrological observations chosen for this study overlap in 2007, and March 2007 mean cloud cover (84%) amounts to the highest cloud cover across the whole Amazon river basin within the January – April 2007 wet season (cloud cover range = 76% - 84%) and is considerably higher than the June – September 2007 dry season cloud cover (46% - 56%).

2.1 Wetland process controls

Wetland CH_4 emissions are controlled by a range of biogeochemical processes: inundation is likely to be a first order control of wetland emissions, as soil CH_4 production largely occurs in oxygen-depleted soils (Whalen et al., 2005). However, extensive studies of wetland CH_4 emissions suggest that inundation is not the sole determinant of spatial and temporal CH_4 emission dynamics. CH_4 can be transferred directly into the atmosphere via macrophytes, thus circumventing the aerobic soil layer (Whalen et al., 2005). Water-body depth (Mitsch et al., 2010), type (Devol et al., 1990) together with aquatic macrophyte density (Laanbroek 2010) can affect the proportion of wetland CH_4 transferred to the atmosphere.

Carbon (C) availability is also a determinant of wetland CH_4 emissions. Methanogen-available C turnover rates (Miyajima et al., 1997), composition (Wania et al., 2010), temporal dynamics (Bloom et al., 2012) and C stocks together drive spatial and temporal variability of carbon limitation on CH_4 production in wetlands. C cycle state variables, including the spatial variability of total biomass (Saatchi et al., 2011; Baccini et al., 2012) and soil carbon (Hiederer and Köchy, 2011) vary at <1000km scales. Methanogen-available C sources – such as gross primary production (GPP) and leaf litter –vary substantially at monthly timescales in the wet tropics (Beer et al., 2010; Chave et al., 2010; Caldararu et al., 2012). In the next section, we establish the CH_4 flux resolution and precision requirements based on the variability of potential tropical wetland CH_4 emissions process controls (namely carbon uptake, live biomass and dead organic matter stocks, inundation and precipitation).

2.2 Wetland CH_4 flux requirements

Here we define a set of wetland CH_4 flux precision and resolution requirements suitable for the formulation and testing of wetland CH_4 emissions process control hypotheses. Measurement and model-based analyses of Amazon wetland CH_4 emissions provide a range of contradictory estimates on spatial patterns and seasonality (Devol et al., 1990; Riley et al., 2011; Bloom et al., 2012; Melton et al., 2013; Basso et al., 2016) suggesting that the basin-wide process controls on wetland

CH_4 emissions remain virtually unknown. Here, our aim is to provide a first order, model-independent characterization of wetland CH_4 flux resolution and precision requirements based on the basin-wide variations in carbon and hydrological processes. Our resolution requirement is based on the correlation lengths of hypothesized wetland CH_4 emission process controls. At the required resolution, our precision requirement is that wetland CH_4 emissions scenarios – derived from a range of hypothesized carbon and hydrological process controls – are (a) statistically inter-distinguishable and (b) distinguishable from a spatio-temporally uniform wetland CH_4 flux (i.e. a null hypothesis).

Given our process-level understanding of wetland CH_4 emissions, we propose four carbon and three hydrological proxies as the dominant drivers of wetland CH_4 emission variability (C1-C4 and H1-H3 respectively). We use carbon stocks and fluxes as proxies for variation in C availability for wetland CH_4 production. We characterize the spatial variability of carbon uptake based on the Jung et al., (2009) eddy-covariance based monthly 0.5° × 0.5° GPP product (C1), and monthly 0.5° × 0.5° solar-induced fluorescence retrieved from the Global Ozone Monitoring Experiment measurements (Joiner et al., 2013; C2). We use the Saatchi et al., (2011) biomass map (C3) and the Hiederer and Köchy, (2011) live biomass and dead organic matter carbon stocks (C4). We define the spatial variability of hydrological controls over methane flux based on two inundation fraction datasets (Prigent et al., 2012; Schroeder et al., 2015; H1 and H2) and the NASA Tropical Rainfall Measuring Mission (TRMM; Huffman et al., 2007) precipitation retrievals (H3).

CH_4 flux resolution

Our resolution requirement is based on a first-order assessment of the process variable correlation length scales: we anticipate that retrieving wetland CH_4 fluxes at much finer scales may be redundant, while retrieving fluxes at much coarser scales may hinder the potential to investigate biogeochemical process controls on wetland CH_4 emission variability. We use an auto-correlative approach to identify the variability length-scales of potential CH_4 emissions process controls (see Appendix A). The spatial auto-correlation coefficients (Moran's I) of the seven limiting process variables indicate coherent spatial structures spanning up to ~ 333km – 666km across the Amazon river basin (Figure 3): process variables exhibit high

auto-correlation at a 1° × 1° resolution (L ~ 111km), and no significant spatial correlation at 6° × 6° (L ~ 666km). Based on our correlative analysis, we expect that wetland CH_4 flux estimates at 3° × 3° (L ~333km) will likely be critical for a first-order distinction between the roles of carbon and water processes on Amazon wetland CH_4 emissions: we propose a ~333km CH_4 flux resolution as the spatial resolution required to determine the role of process control variability on wetland CH_4 emissions. For all time-varying datasets (C1, C4, H1, H2 and H3), we conducted a lagged Pearson's correlation analysis: the time varying datasets indicate varying levels of statistically significant 1-month auto-correlations across the study region (percent of area exhibiting significant autocorrelations: C1 = 98%; C4 = 6%; H1 = 47%; H2 = 51%; H3 = 64%), while virtually 0% of the study region exhibits significant 2-months temporal auto-correlations. For this study, we opt for a monthly temporal resolution requirement: however, we note that higher-temporal resolution datasets (given their availability) can potentially provide an improved assessment of the temporal correlation scales of carbon and hydrological process controls.

CH_4 flux precision

We next derive the CH_4 flux precision required to distinguish between hypothesized wetland CH_4 process controls at a ~333km monthly resolution. We derive the precision requirements assuming one continuous year of CH_4 flux retrievals. We formulate (a) spatial CH_4 emission hypotheses, where wetland CH_4 emissions linearly co-vary with the hypothesized processes at ~333km scales, and (b) temporal CH_4 emission hypotheses, where wetland CH_4 emissions linearly co-vary with the hypothesized processes on monthly timescales scales. Our motivation for evaluating both spatial and temporal hypotheses is that we do not necessarily expect the spatial and temporal process controls on wetland CH_4 emissions to be the same. For example, Amazon wetland CH_4 emissions could be spatially limited by carbon uptake (GPP) and temporally driven by inundation. Each wetland hypothesis is scaled to an annual mean flux of 12 mg m^{-2} day^{-1}, which corresponds to the Melack et al., (2004) annual Amazon-wide wetland CH_4 emission estimate (29.3 Tg CH_4 yr^{-1} across 668 Mha). The explicit formulation of spatial and temporal wetland CH_4 emission hypotheses is described in Appendix B.

For a range of retrieved CH_4 flux precisions across the Amazon basin (spanning 1 – 100 mg m^{-2} day^{-1}), we test whether each spatial and temporal wetland CH_4 emission hypothesis is statistically distinct from alternative hypotheses and a "no variability" hypothesis (i.e. a null hypothesis); the derivation of the statistical confidence in distinguishing between hypotheses is described in Appendix B. The distinction confidence (%) for spatial and temporal hypotheses is shown in Figure 4: at a monthly ~333km resolution, both spatial and temporal wetland CH_4 emission hypotheses are inter-distinguishable with >95% confidence at a ≤ 10 mg m^{-2} day^{-1} CH_4 flux precision.

CH_4 requirements

Given the spatial and temporal variability of potential hydrological and carbon controls, we define the following requirements for wetland CH_4 flux retrievals:

- CH_4 flux spatial resolution = ~333km
- CH_4 flux temporal resolution: monthly
- CH_4 flux precision: = 10 mg CH_4 m^{-2} day^{-1}

Our resolution and precision requirements provide a first-order assessment of the wetland CH_4 emission biogeochemical process control variability. We anticipate that satellite-based CH_4 flux estimates meeting the above-stated requirements will provide robust characterization of spatial variation in Amazon wetland CH_4 emissions on the scale of variation in the major carbon and water controls, allowing forcing (hydrology and carbon) and response (CH_4 flux) to be related directly. Therefore, by retrieving CH_4 fluxes at the required resolution and precision, carbon and hydrological process hypotheses on the dominant drivers of Amazon wetland CH_4 emissions can be adequately investigated. However, depending on the nature of the scientific investigation, we recognize that the trade-off space between spatial resolution, temporal resolution, precision and study duration can be further explored to derive an optimal combination of CH_4 flux requirements.

Throughout the next subsections, we characterize the required satellite column CH_4 measurements needed to resolve CH_4 flux with the above-stated requirements. To quantify the sensitivity of our results to the above-mentioned requirements, we repeat our analysis for a range of CH_4 flux spatial resolution requirements (L = 150km – 990km) and we derive the corresponding CH_4 flux precision requirements.

2.3 CH_4 observation requirements

We define the atmospheric CH_4 observation requirements by retrieving CH_4 fluxes from a range of low-earth orbit (LEO), and geo-stationary orbit (GEO) OS simulated CH_4 retrieved concentrations, or "observations". Our approach is three-fold: (a) we simulate LEO and GEO CH_4 observations for March 2007; (b) we derive the precision of CH_4 measurement averaged at an $L \times L$ resolution (henceforth the "cumulative CH_4 measurement precision"), and (c) we employ an idealized inversion to simulate CH_4 flux retrieval uncertainty for March 2007 based on the cumulative CH_4 measurement precision. We note that wetland emissions are the largest and most uncertain source of CH_4 within the Amazon river basin (Wilson et al., 2016; Melton et al., 2013). We henceforth assume that the non-wetland CH_4 contribution (namely fires and anthropogenic CH_4 sources) can be relatively well characterized using ancillary datasets and global inventories (Bloom et al., 2015; Turner et al., 2015 and references therein).

LEO and GEO CH_4 observations

The advantage of LEO systems is a near-global coverage; for the TROPOMI mission CH_4 orbit and measurement parameters, this equates to a 1-day maximum re-visit period globally. While a GEO system can only view a fixed area on the globe, revisit periods can be far shorter. To relate CH_4 observation requirements to current technological capabilities, we explore six OS configurations based on LEO and GEO OS parameters used to simulate the up-coming GEOCAPE and TROPOMI missions' observations in North America by Wecht et al., (2014) (Table 1). We note that, for regional CH_4 emission estimates, the GEO OS configurations are expected outperform LEO due to a larger data volume: the fixed viewing

area permits multiple re-visits per day (Wecht et al., 2014), and the smaller GEO footprint size typically leads to lower cloud-contamination (Crisp et al., 2004). Our aim here is not to compare CH_4 emission estimates from LEO and GEO CH_4 retrievals. Rather, our aim is to determine whether CH_4 emission estimates from a range of LEO and GEO OS configurations are able meet the wetland process requirements outlined in section 2.1.

Cloud cover is a major limiting factor in Amazon basin trace-gas retrievals. Mean March 2007 cloud cover is 89% – ranging from 38% to 98% at a 1° × 1° resolution – throughout the Amazon river basin (based on MODIS cloud-cover data, Figure B1). We quantify the data-rejection due to cloud cover based on 1km March 2007 MODIS cloud cover data. Based on four MODIS cloud cover flags, we categorize 1km × 1km cloud-cover observations into "cloud-contaminated" and "cloud free" observations (see Appendix C). Any cloud-contaminated 3km×3km (GEO) or 7km×7km (LEO) CH_4 measurement footprints are rejected, i.e. all accepted footprints are 100% "cloud-free".

To assess the relative importance of CH_4 measurement density in high cloud-cover areas, we test two additional geo-stationary configurations: "GEO-Z1" carries out two visits per day and 6 visits per day in the top 50% cloudiest areas; "GEO-Z2" carries out two visits per day and 10 visits per day in the top 25% cloudiest areas (we note that these two OS would require targeting capabilities to optimize the sampling strategy over the cloudiest area of the basin). We further explore OS space by testing LEO with a $\sqrt{2}$ precision enhancement ("LEO+") and GEO with 8 visits per day instead of 4 ("GEO×2").

Cumulative CH_4 measurement precision

For each OS ω ("GEO","LEO", etc.), $\mathbf{O}^{\{L,\omega\}}$ is the cumulative CH_4 measurement precision at a $L \times L$ resolution. $\mathbf{O}^{\{L,\omega\}}$ is an $N \times 1$ array, where N is the number of Amazon river basin grid-cells at resolution $L \times L$. We derive the cumulative atmospheric CH_4 precision within each $L \times L$ grid-cell i, $O_i^{\{L,\omega\}}$ as follows:

$$O_i^{\{L,\omega\}} = \frac{\sigma_\omega}{\sqrt{a\,\phi_i^{\{\omega\}}\,n^{\{\omega\}}\,L^2}} \qquad (1)$$

where σ_ω is the single observation precision (table 1), $\phi_i^{\{\omega\}}$ is the fraction of cloud-free observations at location i, $n^{\{\omega\}}$ is the number of observations per km^2 per month for OS ω (based on Table 1 values), and a the fraction of accepted cloud-free CH_4 column retrievals (set to a = 0.5); The derivation of $\phi_i^{\{\omega\}}$ is based on MODIS 1-km cloud cover data over the Amazon river basin in March 2007 (Appendix C). The square of the denominator in (1) corresponds to the number of atmospheric column CH_4 measurements per $L \times L$ grid-cell. For all OS, $n^{\{\omega\}}$ is calculated assuming continuous basin-wide coverage at the single-sounding footprint resolution (see Table 1). We highlight that our formulation of cumulative CH_4 precision in equation 1 implies retrieved CH_4 errors are spatially and temporally uncorrelated.

OS retrieved CH_4 flux precision

We calculate the monthly retrieved CH_4 flux precision for OS ω at an $L \times L$ resolution – $\mathbf{F}^{\{L,\omega\}}$ –based on $\mathbf{O}^{\{L,\omega\}}$ (equation 1). $\mathbf{F}^{\{L,\omega\}}$ is a $N \times 1$ array, where N is the number of Amazon basin grid-cells at resolution $L \times L$. To calculate $\mathbf{F}^{\{L,\omega\}}$ we simulate an ensemble of 1000 retrieved CH_4 concentrations vectors ($\mathbf{c}_{*,n}^{\{L,\omega\}}$ for n = 1 – 1000) over the Amazon river basin, where:

$$\mathbf{c}_{*,n}^{\{L,\omega\}} = \mathbf{c}^{\{L,0\}} + \mathbf{N}(0,1) \circ \mathbf{O}^{\{L,\omega\}}; \qquad (2)$$

$\mathbf{c}^{\{L,0\}}$ is a $N \times 1$ array of $L \times L$ gridded unperturbed CH_4 concentrations, $\mathbf{N}(0,1)$ is an $N \times 1$ array of normally distributed random numbers with mean zero and variance one ("∘" denotes element-wise multiplication). We relate the concentrations $\mathbf{c}^{\{L,*\}}$ to the underlying CH_4 fluxes $\mathbf{f}^{\{L,*\}}$ as follows:

$$\mathbf{c}^{\{L,*\}} = \mathbf{A}^{\{L\}}\mathbf{f}^{\{L,*\}}, \qquad (3)$$

where $\mathbf{A}^{\{L\}}$ is the atmospheric transport operator (the $N \times N$ matrix transforming fluxes to concentrations over the Amazon river basin domain) and $\mathbf{f}^{\{L,*\}}$ is an $N \times 1$ array of surface CH_4 fluxes. For the sake of brevity, we present a summary of $\mathbf{A}^{\{L\}}$ here, and the complete derivation of $\mathbf{A}^{\{L\}}$ in Appendix D. We use a Lagrangian Particle Dispersion Model (LPDM: Uliasz, 1994; Lauvaux and Davis, 2014) to derive an "influence function" (or "column footprint") relating satellite-retrieved atmospheric CH_4 concentrations to surface fluxes (the inverse solution of the transport from the surface to higher altitudes) at the center of the study area. We simulate 30km × 30km CH_4 transport – $\mathbf{A}^{\{30\text{km}\}}$ – by spatially translating the LPDM influence function throughout the domain. To assess the robustness of the LPDM approach, we also simulated CH_4 column mixing ratios over the Amazon river basin at 30km using the Weather Research and Forecasting model (WRF v2.5.1, Skamarock et al., 2008). The WRF model March 2007 Amazon river basin concentrations and the corresponding LPDM approximations are shown in Figure D1. Finally, we used a Monte Carlo approach to statistically construct $\mathbf{A}^{\{L\}}$ based on $\mathbf{A}^{\{30\text{km}\}}$. The LPDM, WRF and the Monte Carlo derivation of $\mathbf{A}$ are fully described in Appendix D.

For each L, we simulate the flux uncertainty based on the inverse of $\mathbf{A}^{\{L\}}$, $(\mathbf{A}^{\{L\}})^{-1}$ and simulated CH_4 concentrations vectors ($\mathbf{c}_{*,n}^{\{L,\omega\}}$, equation 2). For the sake of simplicity, we set all unperturbed concentrations – $\mathbf{c}^{\{L,0\}}$ in equation 2 – to be equal to zero, since these do not influence our subsequent derivation of $\mathbf{F}^{\{L,\omega\}}$. The n^{th} retrieved flux estimate – $\mathbf{f}_{*,n}^{\{L,\omega\}}$ – is calculated as:

$$\mathbf{f}_{*,n}^{\{L,\omega\}} = (\mathbf{A}^{\{L\}})^{-1}\,\mathbf{c}_{*,n}^{\{L,\omega\}}. \quad (4)$$

Finally, we calculate the flux precision $\mathbf{F}^{\{L,\omega\}}$ at grid-cell i as follows:

$$F_i^{\{L,\omega\}} = StDev\left(\mathbf{f}_{i,*}^{\{L,\omega\}}\right). \quad (5)$$

Residual CH_4 bias simulation

Despite the implementation of CH_4 bias correction methods based on satellite CH_4 retrieval comparison against ground measurements of total column CH_4 (Parker et al., 2011), spatial structures in residual CH_4 biases are a key limiting factor in top-down CH_4 flux accuracy. Here we quantify the role residual CH_4 biases for each OS configurations. We simulate a retrieved pseudo-random CH_4 bias structure with a spatial correlation of s = 100km and no temporal correlation, which is consistent with the likely first order predictors of retrieved CH_4 residual biases (Worden et al., 2016). Here we simulate a range of pseudo-random bias distributions with standard deviations spanning b = 0.5 – 50ppb. For each b, we calculate the bias-influenced flux uncertainty $\mathbf{F}^{\{L,\omega,b\}}$ based on equations 4 and 5: to incorporate spatially correlated biases, we adapt eq. 2 to derive the mean concentration uncertainty $\mathbf{c'}^{\{L,\omega,b\}}_{*,n}$ as

$$\mathbf{c'}^{\{L,\omega,b\}}_{*,n} = \mathbf{N}(0,1) \cdot \mathbf{O}^{\{L,\omega\}} + \mathbf{N}(0,1) \cdot b \cdot \frac{s}{L\sqrt{v}} \quad (6)$$

where b represents the standard deviation of the pseudo-random CH_4 bias, v represents the number of visits per month; for bias errors correlated across spatial scales s, the scale factor $\frac{s}{L\sqrt{v}}$ accounts for the pseudo-random behaviour of bias errors b at a monthly $L \times L$ resolution. We assess the role CH_4 biases on $\mathbf{F}^{\{L,\omega,b\}}$ for the LEO and GEO OS configurations at L = ~333km.

3. Results and Discussion

Cumulative CH_4 precision for mean monthly atmospheric column CH_4 measurements is 0.10 – 0.98 ppb for the LEO OS (Figure 5, left) and 0.02 – 0.20 ppb for the GEO OS (Figure 5, right). The lowest CH_4 concentration precision occurs in the East and central Amazon river basin. A crucial advantage of the smaller GEO OS footprint is the 88–148% higher probability of cloud-free observations in the cloudiest regions of the Amazon river basin (Figure B1); the probability of

acquiring cloud-free observations in cloud-prone areas is further enhanced by the GEO OS ability to conduct multiple visits per day (see eq. 1).

For L = ~333km, median monthly retrieved CH_4 flux precision for the LEO OS (i.e. the median of $\boldsymbol{F}^{\{L,\omega\}}$) is 17.0 mg CH_4 m^{-2} day^{-1} (Figure 6); increasing the single sounding retrieval precision by $\sqrt{2}$ (from 0.6ppb to 0.42ppb) for LEO observations (LEO+) reduces the retrieved flux uncertainty to 11.9 mg CH_4 m^{-2} day^{-1}. This uncertainty reduction is equivalent to a second LEO visit per day (see table 1): the factor 3-to-10 lower uncertainties for cumulative GEO CH_4 concentrations (Figure 5) lead to a 2.7 mg CH_4 m^{-2} day^{-1} median uncertainty in the retrieved flux (Figure 6). Doubling the number of GEO visits per day (GEOx2 OS) reduces the retrieved flux uncertainty to 1.9 mg CH_4 m^{-2} day^{-1}. GEO-Z1 and GEO-Z2 uncertainties (2.4 and 2.0 mg CH_4 m^{-2} day^{-1}) are both lower than GEO. These results indicate that – despite a lower number of accepted observations – a higher observation density in the high cloud-cover areas of the Amazon basin (and lower observation density elsewhere) can be used to reduce the retrieved CH_4 flux uncertainty without increasing the number of observations per day. Based on the LEO OS, we anticipate that missions similar to the ESA TROPOMI observation configuration (Veefkind et al., 2012; Wecht et al., 2014) will lead to lower-than-required information content for Amazon wetlands and are unlikely to provide sufficient observational constraints to resolve the dominant CH_4 flux processes.

Our bias CH_4 analysis (Figure 7) indicates that GEO retrieved CH_4 flux precisions at L = ~333km are relatively unaffected by residual CH_4 biases <1ppb, while LEO retrieved CH_4 flux precisions are relatively unaffected by residual CH_4 biases ≤5ppb. We find that the advantage of GEO CH_4 flux precision over LEO diminishes from almost one order of magnitude at residual CH_4 biases <1ppb, to roughly a factor of 2 for residual biases >20ppb. Here we assume a residual CH_4 bias correlation scale of 100km (section 2.3); based on eq. 6, we expect a larger impact of residual CH_4 biases on OS retrieved CH_4 flux precision for residual CH_4 bias correlation lengths >100km or for temporally correlated CH_4 biases. Overall, the relative advantage of GEO over LEO OSs is contingent on both the cumulative CH_4 precision (Figure 5) as well as the anticipated spatiotemporal structure of residual CH_4 bias.

Estimates of fluxes at L = 150 – 990km show that median GEO retrieved CH_4 flux uncertainty is consistently a factor of ~5 lower than the median LEO retrieved CH_4 flux uncertainty (Figure 8); for a 10ppb residual pseudo-random bias, the median GEO retrieved flux uncertainty is consistently a factor of ~3 lower than LEO-retrieved flux uncertainty. GEO-derived CH_4 fluxes meet the both the precision and resolution requirements for L = ~180 – 333km; for a 10ppb residual bias, GEO-derived CH_4 fluxes meet both requirements at L = ~280 – 333km. At the expense of the resolution requirement, both GEO simulations meet the precision requirements for all $L \geq$ ~333 km. Unbiased median LEO-derived CH_4 fluxes meet the precision requirements at L>500km; LEO-derived CH_4 fluxes with a 10ppb pseudo-random bias meet the precision requirement at L>800km and partially meet the precision requirement for 550km>L>800km.

In our analysis we have assumed (i) no systematic biases in our atmospheric inversion simulation, and (ii) perfectly known boundary conditions. Significant systematic atmospheric CH_4 retrieval and transport model biases can undermine the enhanced accuracy of geostationary OSs. For example, we find that our LPDM-derived transport operator yields a conservative estimate of the monthly mean CH_4 gradient across the domain relative to the WRF model simulation (Appendix D; Figure D1). We assess the sensitivity of our results to a factor of 1.5 increase in the LPDM-derived transport operator ($\mathbf{A}^{\{L\}}$); OS CH_4 flux precision results exhibit an inversely proportional response, corresponding to a ~33% uncertainty reduction (median GEO flux precision of 1.8 mg CH_4 m^{-2} day^{-1} and a LEO precision of 11.3 mg CH_4 m^{-2} day^{-1}). GEO missions are likely to provide a higher volume of observations at the boundaries of the observation domain, relative to LEO OS: therefore, boundary conditions are likely to reinforce the potential of GEO OS compared to LEO. We recognize that further efforts are required to fully assess the role of seasonal transport variability, transport errors, boundary condition assumptions and atmospheric CH_4 bias structures on the accuracy of GEO and LEO CH_4 flux retrievals.

We note that a limiting factor in our analysis is the lack of data constraints on diurnal cloud-cover variability (since the MODIS cloud cover dataset does not provide diurnal constraints). The March 2007 ERA-interim monthly mean 3h cloud cover dataset indicates a 7 – 80% (median 29%) coefficient of variation of cloud-free fraction diurnal variability throughout the Amazon basin. Given the non-linear sensitivity of data yield to synoptic cloud cover (Figure B1), the cloud-free fraction

coefficient of variation may amount to an important component in assessing and optimizing the performance of LEO and GEO OSs over the Amazon basin, as well as other high cloud-cover regions across the globe.

Our CH_4 flux resolution requirement (monthly L = ~333km CH_4 flux retrievals) is derived based on an assessment of carbon and hydrological auto-correlation scales across the Amazon river basin. Although our sensitivity analysis (Figure 8) shows that GEO can potentially distinguish between the hypothesized CH_4 emission scenarios at L > ~333km, we anticipate that additional biogeochemical investigations – such as the second-order interactions between carbon and hydrological drivers on wetland CH_4 emissions – would likely be increasingly challenging at coarser resolutions. We recognize that our resolution requirement and our quantification of correlation scales is specific to our study region: for example, quantification of greenhouse gas measurement requirements for finer-scale studies would yield a unique set of requirements, and supporting analyses may require higher-resolution datasets. Our approach provides the means to examine trade-offs between spatial and temporal resolutions. For example, further analyses can be conducted to establish the space-time trade-offs to optimize biogeochemical investigations and process uncertainty reduction. We also note that GEO OSs provide unprecedented volume of observations: the enhanced sampling approach can potentially be used at shorter timescales to optimally resolve source and transport patterns. This approach could be particularly useful in instances wetland CH_4 emissions are densely focused in space or time. Finally, we highlight the potential for combining multiple OSs (e.g. LEO and GEO systems) to optimally constrain CH_4 fluxes and biogeochemical process controls; the potential of OS synergies undoubtedly requires further investigation.

In contrast to our approach, CH_4 flux uncertainty requirements can alternatively be derived by quantifying process-based wetland CH_4 emission model uncertainty (Melton et al., 2013), or by characterizing the CH_4 flux uncertainty stemming from wetland CH_4 model parametric uncertainty (Bloom et al., 2012). An advantage of model-based requirements is the ability to assess CH_4 flux uncertainties associated with the complex interactions between wetland CH_4 processes (e.g. Riley et al., 2011). Prior information on the magnitude and variability of fluxes can also be introduced (e.g. in a Bayesian atmospheric transport and chemistry inversion framework) to re-assess posterior uncertainty estimates.

However, as outlined in section 2.1, large unknowns preside over the processes governing the spatial and temporal variability of wetland CH_4 fluxes. Moreover, wetland CH_4 models often exhibit structural similarities (Melton et al., 2013); for example, wetland CH_4 emission models (Melton et al., 2013) suggest major CH_4 emissions along the main stem of the Amazon river (Figure 1). Since model spatiotemporal CH_4 flux variations – and their associated processes – have not been adequately assessed due to insufficient in-situ measurements (particularly in the tropics), the introduction of prior spatial and temporal correlations in wetland CH_4 flux estimates would hinder the potential to independently investigate biogeochemical process controls on wetland CH_4 emissions. To our knowledge, our analysis provides a first quantification of the OS requirements for confronting prior knowledge on CH_4 fluxes at a process-relevant resolution.

4. Concluding remarks

Quantitative knowledge of biogeochemical processes controlling biosphere-atmosphere greenhouse gas fluxes remains highly uncertain. Optimally designed satellite greenhouse gas observing systems can potentially resolve the processes controlling critical boreal and tropical greenhouse gas fluxes. In this study, we have characterized a satellite OS able to resolve the principal process controls on Amazon river basin wetland CH_4 emissions. Conventional low-earth orbit satellite missions will likely be unable to resolve Amazon wetland CH_4 emissions at a process-relevant scale and precision. Observation density in time and space, and its reduction by cloud cover are the major limiting factors. Increasing the number of daily CH_4 measurements in cloudy regions at the expense of other measurements can further reduce the retrieved CH_4 flux precision from geostationary satellite CH_4 measurements. OSSEs based on reducing process uncertainty can inform observation requirements for future greenhouse gas satellite missions in a far more targeted way than simply quantifying overall flux uncertainty reduction for a given OS.

Appendix A: Correlation lengths

All datasets described in section 2.2 were aggregated to a common 0.5° × 0.5° resolution. For each process control dataset, we derive the Moran's I spatial auto-correlation coefficient (r_{MI}) at an $L \times L$ resolution, where L = 0.5°, 1°, 1.5°, … , 10°. For every L we aggregated the dataset to $L \times L$ resolution. To determine whether the derived r_{MI} are significant relative to the null hypothesis, we repeat the Moran's I derivation 2000 times for normally distributed random numbers (in the place of the $L \times L$ gridded dataset), which together statistically represent the Moran's I distribution ($\mathbf{R}_{MI}$) for statistically insignificant spatial correlation. When r_{MI} > median($\mathbf{R}_{MI}$), the r_{MI} p-value is twice the fraction of instances where $\mathbf{R}_{MI} > r_{MI}$; when $r_{MI} \leq$ median($\mathbf{R}_{MI}$), the r_{MI} p-value is twice the fraction of instances where $\mathbf{R}_{MI} < r_{MI}$. A p-value ≥ 0.05 indicates that the null hypothesis cannot be rejected with a 95% confidence.

Appendix B: Spatial and temporal wetland CH_4 emission hypotheses

Detectability of wetland CH_4 hypotheses

Based on the four carbon and three hydrological proxies (see section 2.2), we formulate spatial and temporal wetland CH_4 emission hypotheses (henceforth **S** and **T** respectively) – at a monthly ~333km × 333km resolution – and determine our ability to statistically distinguish between these at a range of retrieved CH_4 flux precisions (p = 1 - 100 mg m^{-2} day^{-1}). For all **S**, we prescribe temporally constant CH_4 emissions and for **T** we annually normalize mean annual emissions to 12 mg m^{-2} day^{-1} within each ~333km × 333km area; For both **S** and **T** we also include a "no variability" scenario, where all emissions in space and time are 12 mg m^{-2} day^{-1}. We note that by minimizing the variability of each hypothesis to a single temporal or spatial variable, we effectively assume a "worst-case" scenario for the detectability **S** and **T** hypotheses relative to the null hypothesis.

For hypothesized process control h we derive the temporal wetland CH_4 emission hypothesis $\mathbf{T}_{*,*,h_2}$ as:

$$T_{x,t,h} = s_x \, P_{x,t,h} \quad \text{(B1)}$$

where $P_{x,t,h}$ represents the hypothesized process control h at location x and time t, and s_x is a scaling factor such that $\overline{\boldsymbol{T}_{x,*,h}}$ = 12 mg m^{-2} day^{-1}. For the temporal hypotheses we omit the soil carbon and carbon stock proxies, as these datasets are not temporally resolved. Each spatial hypothesis $\mathbf{S}_{*,*,h}$ is defined as

$$S_{x,t,h} = s\,\overline{\boldsymbol{P}_{\boldsymbol{x},*,h}} \quad \text{(B2)}$$

where s is a scaling factor such that $\overline{\mathbf{S}_{*,t,h}}$ = 12 mg m^{-2} day^{-1}. For each hypothesis h and each precision p we simulate retrieved CH_4 fluxes $F_{x,t,h,p}$ as

$$F_{x,t,h,p} = H_{x,t,h} + N(0,1) \cdot p \quad \text{(B3)}$$

where $H_{x,t,h}$ is the spatial or temporal hypothesis CH_4 flux ($T_{x,t,h}$ or $S_{x,t,h}$) and N(0,1) is a normally distributed number with mean 0 and variance of 1. For each h, we compare $\mathbf{F}_{*,*,h,p}$ against all hypothesized process controls h' as follows:

$$J_{h,h',p} = \sum_{x,t}(F_{x,t,h,p} - H_{x,t,h'})^2 \quad \text{(B4)}$$

We repeat the derivation of $\mathbf{J}$ 500 times, and we define the detectability confidence $C_{h,p}$ as the percentage of times where $J_{h,h,p}$ = min($\mathbf{J}_{h,*,p}$); the min() function denotes the minimum of all $\mathbf{J}_{h,*,p}$ elements. In summary, $C_{h,p}$ is the probability of distinguishing a hypothesized wetland CH_4 process control h from alternative wetland CH_4 process controls when wetland CH_4 fluxes are retrieved with precision p. $C_{h,p}$ values for spatial and temporal wetland CH_4 hypotheses are summarized in Figure 4. We henceforth define a wetland CH_4 hypothesis as "distinguishable" from alternative hypotheses at precision p when $C_{h,p}$ > 95%.

Appendix C: MODIS cloud cover

The MODIS cloud cover analysis was performed based on the MOD06_L2 1km cloud mask product (downloaded from modis.gsfc.nasa.gov). We consider "probably cloudy" and "cloudy" 1km × 1km pixel flags as cloud-covered areas (CC = 1), and the remaining pixel flag categories ("probably clear" and "clear") as cloud-free areas (CC=0): here we assume that the statistical patterns of cloud-cover across the Amazon domain remain well characterized when assigning "probably clear" and "probably cloudy" pixels to the "cloud-free" and "cloud-covered" categories. We aggregate the 1km data to *N*km × *N*km (*N* is the OS footprint resolution; GEO N = 3km; LEO N = 7km; see Table 1) to calculate the number of cloud-free *N*km × *N*km areas within each MODIS cloud cover scene. The monthly fraction of cloud-free observations $\phi_i^{\{\omega\}}$ (see equation 1) is calculated by deriving the ratio of cloud-free to total *N*km × *N*km areas within each $L \times L$ area. A regional summary of the observation yields (% of cloud-free *N*km × *N*km areas) for a range of footprint resolutions (N = 1 – 10km) is shown in Figure B1.

Appendix D: Atmospheric transport operator

For L = 150km - 990km, we derive the $N \times N$ atmospheric transport operator $\mathbf{A}^{\{L\}}$ for $L \times L$ resolution fluxes based on N random CH_4 flux vectors ($\mathbf{f}'^{\{L\}}$) and their corresponding concentrations ($\mathbf{c}'^{\{L\}}$): $\mathbf{f}'^{\{L\}}$ and $\mathbf{c}'^{\{L\}}$ are $N \times N$ arrays, where each column of $\mathbf{f}'^{\{L\}}$ is a vector of randomly sampled CH_4 fluxes throughout the domain, and each column in $\mathbf{c}'^{\{L\}}$ is a vector of the corresponding CH_4 concentrations. $\mathbf{A}^{\{L\}}$ is derived as:

$$\mathbf{A}^{\{L\}} = \left(\mathbf{f}'^{\{L\}}\right)^{-1}\mathbf{c}'^{\{L\}}. \quad \text{(D1)}$$

For each n, random CH_4 fluxes at grid-cell i are derived as $f_{i,n}'^{\{L\}} = \mathrm{R}(0,1)$, where R(0,1) is a random number sampled from a normal distribution with mean zero and variance 1. Atmospheric concentrations are firstly simulated at resolution L_0 = 30km;

the fluxes $\mathbf{f}_{*,n}^{\prime\{L\}}$ are downscaled to $L_0 \times L_0$ resolution ($\mathbf{f}_{*,n}^{\prime\{L_0\}}$). For each 30km × 30km grid-cell i, the mean atmospheric CH_4 concentration $c_i^{\{L_0\}}$ is calculated as

$$c_{i,n}^{\prime\{L_0\}} = \mathbf{I}_i \mathbf{f}_{*,n}^{\prime\{L_0\}} \qquad \text{(D2)}$$

where $\mathbf{f}_{*,n}^{\{L_0\}}$ is the N × 1 array of CH_4 fluxes, $\mathbf{I}_i$ is the N × 1 influence function array for grid-cell i. We derive $\mathbf{I}_i$ using a Lagrangian Particle Dispersion Model (LPDM, Uliasz, 1994). The influence function derivation (i.e. the column sensitivity to the surface fluxes) is described in Lauvaux and Davis (2014). The influence function was computed for an averaged column observation in the model of the simulation domain, for every hour of March 2007. The inverse calculation of surface fluxes requires the use of the adjoint of the transport at the mesoscale (~2000km). Here, we only simulated the fraction of the column influenced by surface fluxes. We assume boundary conditions are well constrained by satellite and surface network measurements: therefore, only the first 6km of the column was described by the particles released backward in the model.

To simulate total column CH_4 retrieval influence functions, we incorporate a mean GOSAT CH_4 retrieved averaging kernel (Parker et al., 2011) for the Amazon river basin region (Figure A1). To minimize the computational cost of simulating atmospheric transport, we (i) derive the influence function for the center of the domain ($\mathbf{I}_0$, Lat = 4.9°S and Lon = 63.8°W), and (ii) we derive $\mathbf{I}_i$ by spatially translating $\mathbf{I}_0$ to gridcell i latitude and longitude coordinates. Finally, we derive mean $L \times L$ resolution concentrations used in equation C1, ($\mathbf{c}_{*,n}^{\prime\{L\}}$), based on the spatial aggregation of $L_0 \times L_0$ resolution concentrations $\mathbf{c}_{*,n}^{\prime\{L_0\}}$.

To assess the viability of our approach, we simulate March 2007 $L_0 \times L_0$ atmospheric concentrations – based on $\mathbf{f}^{\{L_0,0\}}$, where for i=1 – N, $f_i^{\{L_0,0\}}$= 12 mg m^{-2} day^{-1} – throughout the Amazon river basin domain using (a) equation D2, and (b) WRF CH_4 atmospheric transport model. In the WRF model, $\mathbf{f}^{\{L_0,0\}}$ was coupled to the atmospheric model through the chemistry modules (WRF-Chem) for passive tracers, as described in Lauvaux et al. (2012). The physics configuration of the

model used Mellor-Yamada-Nakanishi-Niino scheme for the Planetary Boundary Layer (Nakanishi and Niino, 2004), the NOAH land surface model (Pan and Mahrt, 1987), the WSM-5 microphysics scheme (Hong et al., 2004), and the Kin-Fritsch cumulus parameterization (Kain, 2004). The meteorological driver data from the Global Forecasting System (FNL) analysis products at 1° × 1° resolution was used at the boundaries of the simulation domain. The simulation domain spans 120x100 $L_0 \times L_0$ grid-points, and 60 vertical levels to describe the atmospheric column up to 50 hPa. The atmospheric column was extracted from the surface to the top of the modeled atmosphere, which represents about 90% of the total air mass. A dilution factor of 0.9 was used to compensate for the partial model column.

The LPDM approach emulates the large-scale WRF CH_4 enhancement ($r^2 = 0.85$ see Figure D1); the smoothing effect is due to the use of a single footprint throughout the entire domain. Mean CH_4 concentrations based on our approach (equation D2) and WRF are 15.23ppb and 17.42ppb respectively. The gradient of CH_4 between the North-East and South-West sub-regions for our approach (equation D2) and WRF are 13.14ppb and 17.24ppb respectively; the delineation of the North-East and South-West domain is shown in Figure D1.

Acknowledgments

Part of this research was carried out at the Jet Propulsion Laboratory, California Institute of Technology, under a contract with the National Aeronautics and Space Administration. Inundation datasets are available at noaacrest.org/rscg/ and wetlands.jpl.nasa.gov. TRMM data is available at mirador.gsfc.nasa.gov. The gross primary production dataset was obtained from bgc-jena.mpg.de. The soil carbon dataset is available at esdac.jrc.ec.europa.eu. ERA-interim synoptic monthly mean re-analyses were downloaded from apps.ecmwf.int.

References

Andrews, A. E., Kofler, J. D., Trudeau, M. E., Williams, J. C., Neff, D. H., Masarie, K. A., Chao, D. Y., Kitzis, D. R., Novelli, P. C., Zhao, C. L., Dlugokencky, E. J., Lang, P. M., Crotwell, M. J., Fischer, M. L., Parker, M. J., Lee, J. T., Baumann, D. D., Desai, A. R., Stanier, C. O., De Wekker, S. F. J., Wolfe, D. E., Munger, J. W., and Tans, P. P.: CO2, CO,

and CH4 measurements from tall towers in the NOAA Earth System Research Laboratory's Global Greenhouse Gas Reference Network: instrumentation, uncertainty analysis, and recommendations for future high-accuracy greenhouse gas monitoring efforts, *Atmos. Meas. Tech.*, 7, 647–687, doi:10.5194/amt-7-647-2014, 2014.

Baccini, A., Goetz, S. J., Walker, W. S., Laporte, N. T., Sun, M., Sulla-Menashe, D., Hackler, J., Beck, P. S. A., Dubayah, R., Friedl, M. A., Samanta, S., and Houghton, R. A.: Estimated carbon dioxide emissions from tropical deforestation improved by carbon-density maps, *Nat. Climate Change*, 2, 182– 185; doi:10.1038/nclimate1354, 2012.

Bacastow, R. B., Adams, J. A., Keeling, C. D., Moss, D. J., Whorf, T. P., and Wong, C. S.: Atmospheric carbon dioxide, the Southern Oscillation, and the weak 1975 El Niño, *Science*, 210, 66–68, doi:10.1126/science.210.4465.66, 1980.

Basso, L. S., Gatti, L. V., Gloor, M., Miller, J. B., Domingues, L. G., Correia, C. S., and Borges, V. F.: Seasonality and interannual variability of CH_4 fluxes from the eastern Amazon Basin inferred from atmospheric mole fraction profiles. *J Geophys Res-Atmos*, 121, 168–184, doi: 10.1002/2015JD023874, 2016.

Beer, C., Reichstein, M., Tomelleri, E., Ciais, P., Jung, M., Carvalhais, N., Rodenbeck, C., Arain, M. A., Baldocchi, D., Bonan, G. B., Bondeau, A., Cescatti, A., Lasslop, G., Lindroth, A., Lomas, M., Luyssaert, S., Margolis, H., Oleson, K. W., Roupsard, O., Veenendaal, E., Viovy, N., Williams, C., Woodward, F. I., and Papale, D.: Terrestrial Gross Carbon Dioxide Uptake: Global Distribution and Covariation with Climate, *Science,* 329, 834– 838, doi:10.1126/Science.1184984, 2010.

Bergamaschi, P., Houweling, S., Segers, A., Krol, M., Frankenberg, C., Scheepmaker, R. A., Dlugokencky, E., Wofsy, S. C., Kort, E. A., Sweeney, C., Schuck, T., Brenninkmeijer, C., Chen, H., Beck, V., and Gerbig, C.: Atmospheric CH_4 in the first decade of the 21st century: Inverse modeling analysis using SCIAMACHY satellite retrievals and NOAA surface measurements, *J. Geophys. Res.*, 118, 7350–7369, doi:10.1002/jgrd.50480, 2013.

Bloom, A. A., Palmer, P. I., Fraser, A., Reay, D. S., and Frankenberg, C.: Large-Scale Controls of Methanogenesis Inferred from Methane and Gravity Spaceborne Data, *Science*, 327, 322–325, doi:10.1126/Science.1175176, 2010.

Bloom, A. A., Palmer, P. I., Fraser, A., and Reay, D. S.: Seasonal variability of tropical wetland CH_4 emissions: the role of the methanogen-available carbon pool, *Biogeosciences*, 9, 2821– 2830, doi:10.5194/bg-9-2821-2012, 2012.

Bloom, A. A., Worden, J., Jiang, Z., Worden, H., Kurosu, T., Frankenberg, C., and Schimel, D.: Remote sensing constraints on South America fire traits by Bayesian fusion of atmospheric and1140 surface data, *Geophys. Res. Lett.*, 42, 1268–1274, doi: 10.1002/2014GL062584, 2015.

Bloom, A. A., Exbrayat, J.-F., van der Velde, I. R., Feng, L., Williams., M. The decadal state of the terrestrial carbon cycle: Global retrievals of terrestrial carbon allocation, pools, and residence times. *P. Natl. Acad. Sci.*, 113, 1285–1290, doi: 10.1073/pnas.1515160113, 2016.

Bousquet, P., Ringeval, B., Pison, I., Dlugokencky, E. J., Brunke, E.-G., Carouge, C., Chevallier, F., Fortems-Cheiney, A., Frankenberg, C., Hauglustaine, D. A., Krummel, P. B., Langenfelds, R. L., Ramonet, M., Schmidt, M., Steele, L. P., Szopa, S., Yver, C., Viovy, N., and Ciais, P.: Source attribution of the changes in atmospheric methane for 2006–2008, *Atmos. Chem. Phys.*, 11, 3689-3700, doi:10.5194/acp-11-3689-2011, 2011.

Bousserez, N., Henze, D. K., Rooney, B., Perkins, A., Wecht, K. J., Turner, A. J., Natraj, V., and Worden, J. R.: Constraints on methane emissions in North America from future geostationary remote sensing measurements, *Atmos. Chem. Phys. Discuss.*, 15, 19017-19044, doi:10.5194/acpd-15-19017-2015, 2015.

Braswell, B. H., Schimel, D. S., Linder, E., & Moore, B. I. I. I.: The response of global terrestrial ecosystems to interannual temperature variability. *Science*, 278, 870-873, doi: 10.1126/science.278.5339.870, 1997.

Butz, A., Guerlet, S., Hasekamp, O., Schepers, D., Galli, A., Aben, I., Frankenberg, C., Hartmann, J.-M., Tran, H., Kuze, A., Keppel-Aleks, G., Toon, G., Wunch, D., Wennberg, P., Deutscher, N., Griffith, D., Macatangay, R., Messerschmidt, J., Notholt, J., and Warneke, T.: Toward accurate CO_2 and CH_4 observations from GOSAT, *Geophys. Res. Lett.*, 38, L14812, doi:10.1029/2011GL047888, 2011.

Butz, A., Galli, A., Hasekamp, O., Landgraf, J., Tol, P., and Aben, I.: TROPOMI aboard Sentinel-5 Precursor: Prospective performance of CH_4 retrievals for aerosol and cirrus loaded atmospheres, *Remote Sens. Environ.*, 120, 267–276, doi:10.1016/j.rse.2011.05.030, 2012.

Caldararu, S., Palmer, P. I., and Purves, D. W.: Inferring Amazon leaf demography from satellite observations of leaf area index, *Biogeosciences*, 9, 1389–1404, doi:10.5194/bg-9-1389- 2012, 2012.

Chave, J., Navarrete, D., Almeida, S., Álvarez, E., Aragão, L.E.O. C., Bonal, D., Châtelet, P., Silva-Espejo, J. E., Goret, J.-Y., von Hildebrand, P., Jiménez, E., Patiño, S. , Peñuela, M. C., Phillips, O. L., Stevenson, P., and Malhi, Y.: Regional and seasonal pat- terns of litterfall in tropical South America, *Biogeosciences*, 7, 43–55, doi:10.5194/bg-7-43-2010, 2010.

Chen, Y., Randerson, J. T., and Morton, C. D.: Tropical North Atlantic ocean-atmosphere interactions synchronize forest carbon losses from hurricanes and Amazon fires. *Geophysical Research Letters*, 42: 6462-6470, doi: 10.1002/2015GL064505, 2015.

Cox, P. M., Pearson, D., Booth, B. B., Friedlingstein, P., Huntingford, C., Jones, C. D., and Luke, C. M.: Sensitivity of tropical carbon to climate change constrained by carbon dioxide variability, *Nature*, 494, 341–344, doi:10.1038/nature11882, 2013.

Crevoisier, C., Nobileau, D., Fiore, A. M., Armante, R., Chédin, A., and Scott, N. A.: Tropospheric methane in the tropics – first year from IASI hyperspectral infrared observations, *Atmos. Chem. Phys.*, 9, 6337-6350, doi:10.5194/acp-9-6337-2009, 2009.

Crisp, D., Atlas, R. M., Breon, F.-M., Brown, L. R., Burrows, J. P., Ciais, P., Connor, B. J., Doney, S. C., Fung, I. Y., Jacob, D. J., Miller, C. E., O'Brien, D., Pawson, S., Randerson, J. T., Rayner, P., Salawitch, R. J., Sander, S. P., Sen, B., Stephens, G. L., Tans, P. P., Toon, G. C., Wennberg, P. O., Wofsy, S. C., Yung, Y. L., Kuang, Z., Chudasama, B., Sprague, G., Weiss, B., Pollock, R., Kenyon, D., and Schroll, S.: The Orbiting Carbon Observatory (OCO) mission, *Adv. Space Res.*, 34, 700–709, doi:10.1016/j.asr.2003.08.062, 2004.

Devol, A. H., Richey, J. E., Forsberg, B. R., and Martinelli, L. A.: Seasonal dynamics in methane emissions from the Amazon River floodplain to the troposphere, *J. Geophys. Res.*, 95, 16417–16426, doi:10.1029/JD095iD10p16417, 1990.

Fox, A., Williams, M., Richardson, A. D., Cameron, D., Gove, J. H., Quaife, T., Ricciuto, D., Reichstein, M., Tomelleri, E., Trudinger, C. M., and Van Wijk, M. T.: The REFLEX project: Comparing different algorithms and implementations for the inversion of a terrestrial ecosystem model against eddy covariance data, *Agr. Forest Meteorol.*, 149, 1597–1615, doi:10.1016/j.agrformet.2009.05.002, 2009.

Frankenberg, C., Bergamaschi, P., Butz, A., Houweling, S., Meirink, J. F., Notholt, J., Petersen, A. K., Schrijver, H., Warneke, T., and Aben, I.: Tropical methane emissions: A re- vised view from SCIAMACHY onboard ENVISAT, *Geophys. Res. Lett.*, 35, L15811, doi:10.1029/2008GL034300, 2008.

Franklin, J., Serra-Diaz, J. M., Syphard, A. D., and Regan, H. M.: Global change and terrestrial plant community dynamics, *P. Natl. Acad. Sci.*, 113, 3725–3734, doi: 10.1073/pnas.1519911113, 2016

Fung, I., John, J., Lerner, J., Matthews, E., Prather, M., Steele, L. P., and Fraser, P. J.: Three-dimensional model synthesis of the global methane cycle, *J. Geophys. Res.*, 96, 13033–13065, doi:10.1029/91JD01247, 1991.

Friedlingstein, P., Meinshausen, M., Arora, V. K., Jones, C. D., Anav, A., Liddicoat, S. K., and Knutti, R.: Uncertainties in CMIP5 climate projections due to carbon cycle feedbacks, *J. Climate*, 27, 511–526, doi:10.1175/JCLI-D-12-00579.1, 2013.

Gurney, K. R., Baker, D., Rayner, P., Denning, S., Law, R., Bousquet, P., Bruhwiler, L., Chen, Y. H., Ciais, P., Fung, I., Heimann, M., John, J., Maki, T., Maksyutov, S., Peylin, P., Prather, M., Pak, B., and S. Taguchi, S.: Interannual variations in continental-scale net carbon exchange and sensitivity to observing networks estimated from atmospheric CO_2 inversions for the period 1980–2005, *Global Biogeochem. Cy.*, 22, GB3025, doi:10.1029/2007GB003082, 2008.

Hong, S., Dudhia, J., and Chen, S.: A revised approach to ice microphysical processes for the bulk parameterization of clouds and precipitation, *Mon. Weather Rev.*, 132, 103–120, 2004.

Hiederer, R. and M. Köchy: Global soil organic carbon estimates and the harmonized world soil database, EUR, 79, 25225, doi:10.2788/13267, 2011.

Huffman, G. J., Bolvin, D. T., Nelkin, E. J., Wolff, D. B., Adler, R. F., Gu, G., Hong, Y., Bowman, K. P., and Stocker, E. F.: The TRMM Multisatellite Precipitation Analysis (TMPA): Quasi-global, multiyear, combined-sensor precipitation estimates at fine scales, *J. Hydrometeorol.*, 8, 38–55, doi:10.1175/JHM560.1, 2007.

Huntzinger, D. N., Post, W. M., Wei, Y., Michalak, A. M., West, T. O., Jacobson, A. R., Baker, I. T., Chen, J. M., Davis, K. J., Hayes, D. J., Hoffman, F. M., Jain, A. K., Liu, S., McGuire, A. D., Neilson, R. P., Potter, C., Poulter, B., Price, D., Raczka, B. M., Tian, H. Q., Thornton, P., Tomelleri, E., Viovy, N., Xiao, J., Yuan, W., Zeng, N., Zhao, M., and Cook, R.:

North American Carbon Project (NACP) Regional Interim Synthesis: Terrestrial Biospheric Model Intercomparison, *Ecol. Model.*, 224, 144–157, doi:10.1016/j.ecolmodel.2012.02.004, 2012.

Joiner, J., Guanter, L., Lindstrot, R., Voigt, M., Vasilkov, A. P., Middleton, E. M., Huemmrich, K. F., Yoshida, Y., and Frankenberg, C.: Global monitoring of terrestrial chlorophyll fluorescence from moderate-spectral-resolution near-infrared satellite mea- surements: methodology, simulations, and application to GOME- 2, *Atmos. Meas. Tech.*, 6, 2803–2823, doi:10.5194/amt-6-2803- 2013, 2013.

Jung, M., Reichstein, M., and Bondeau, A.: Towards global empirical upscaling of FLUXNET eddy covariance observations: validation of a model tree ensemble approach using a biosphere model, *Biogeosciences*, 6, 2001-2013, doi:10.5194/bg-6-2001-2009, 2009.

Laanbroek, H. J.: Methane emission from natural wetlands: interplay between emergent macrophytes and soil microbial processes, A mini-review, *Ann. Bot.-London*, 105, 141–153, 2010.

Kain, J. S.: The Kain–Fritsch Convective Parameterization: An Update, *J. Appl. Meteorol.*, 43, 170–181, doi:10.1175/1520-0450(2004)043<0170:TKCPAU>2.0.CO;2, 2004.

King, A. W., Andres, R. J., Davis, K. J., Hafer, M., Hayes, D. J., Huntzinger, D. N., de Jong, B., Kurz, W. A., McGuire, A. D., Vargas, R., Wei, Y., West, T. O., and Woodall, C. W.: North America's net terrestrial CO2 exchange with the atmosphere 1990–2009, *Biogeosciences*, 12, 399-414, doi:10.5194/bg-12-399-2015, 2015.

Kirschke, S., Bousquet, P., Ciais, P., Saunois, M., Canadell, J. G., Dlugokencky, E. J., Bergamaschi, P., Bergmann, D., Blake, D. R., Bruhwiler, L., Cameron-Smith, P., Castaldi, S., Chevallier, F., Feng, L., Fraser, A., Heimann, M., Hodson, E. L., Houweling, S., Josse, B., Fraser, P. J., Krummel, P. B., Lamarque, J.- F., Langenfelds, R. L., Le Quéré, C., Naik, V.,

O'Doherty, S., Palmer, P. I., Pison, I., Plummer, D., Poulter, B., Prinn, R. G., Rigby, M., Ringeval, B., Santini, M., Schmidt, M., Shindell, D. T., Simpson, I. J., Spahni, R., Steele, L. P., Strode, S. A., Sudo, K., Szopa, S., van der Werf, G. R., Voulgarakis, A., van Weele, M., Weiss, R. F., Williams, J. E., and Zeng, G.: Three decades of global methane sources and sinks, *Nat. Geosci.*, 6, 813–823, doi:10.1038/ngeo1955, 2013.

Lauvaux, T., Schuh, A. E., Uliasz, M., Richardson, S., Miles, N., Andrews, A. E., Sweeney, C., Diaz, L. I., Martins, D., Shepson, P. B., and Davis, K. J.: Constraining the CO2 budget of the corn belt: exploring uncertainties from the assumptions in a mesoscale inverse system, *Atmos. Chem. Phys.*, 12, 337-354, doi:10.5194/acp-12-337-2012, 2012.

Lauvaux, T. and Davis, K. J.: Planetary boundary layer errors in mesoscale inversions of column-integrated CO_2 measurements, *J. Geophys. Res.-Atmos.*, 119, 490–508, doi:10.1002/2013jd020175, 2014.

Lee, J.-E., Frankenberg, C., van der Tol, C., Berry, J. A., Guanter, L., Boyce, C. K., Fisher, J. B., Morrow, E., Worden, J. R., Asefi, S., Badgley, G., and Saatchi, S.: Forest productivity and water stress in Amazonia: observations from GOSAT chlorophyll fluorescence, *Proc. R. Soc. B*, 280, 20130171, doi:10.1098/rspb.2013.0171, 2013.

Marengo, J. A., Alves, L. M., Soares, W. R., Rodriguez, W. R., Camargo, H., Paredes Riveros, M., and Diaz Pabló, A.: Two Contrasting Severe Seasonal Extremes in Tropical South America in 2012: Flood in Amazonia and Drought in Northeast Brazil. J. Climate, 26, 9137–9154, doi: 10.1175/JCLI-D-12-00642.1, 2013.

Melack, J. M., Hess, L. L., Gastil, M., Forsberg, B. R., Hamilton, S. K., Lima, I. B. T., and Nova, E. M. L. M.: Regionalization of methane emissions in the Amazon basin with microwave remote sensing, *Global Change Biol.*, 10, 530–544, 2004.

Melton, J. R., Wania, R., Hodson, E. L., Poulter, B., Ringeval, B., Spahni, R., Bohn, T., Avis, C. A., Beerling, D. J., Chen, G., Eliseev, A. V., Denisov, S. N., Hopcroft, P. O., Lettenmaier, D. P., Riley, W. J., Singarayer, J. S., Subin, Z. M., Tian, H., Zürcher, S., Brovkin, V., van Bodegom, P. M., Kleinen, T., Yu, Z. C., and Kaplan, J. O.: Present state of global wetland extent and wetland methane modelling: conclusions from a model inter-comparison project (WETCHIMP), *Biogeosciences*, 10, 753-788, doi:10.5194/bg-10-753-2013, 2013.

Mitsch, W., Nahlik, A., Wolski, P., Bernal, B., Zhang, L., and Ram- berg, L.: Tropical wetlands: seasonal hydrologic pulsing, carbon sequestration, and methane emissions, *Wetlands Ecol. Manage.*, 18, 573–586, doi:10.1007/s11273-009-9164-4, 2010.

Miyajima, T., Wada, E., Hanba, Y. T., and Vijarnsorn, P.: Anaerobic mineralization of indigenous organic matters and methanogene- sis in tropical wetland soils, *Geochimica et Cosmochimica Acta*, 61, 3739–3751, doi:10.1016/S0016-7037(97)00189-0, 1997.

Myhre, G., Shindell, D., Bréon, F.-M., Collins, W., Fuglestvedt, J., Huang, J., Koch, D., Lamarque, J.-F., Lee, D., Mendoza, B., Nakajima, T., Robock, A., Stephens, G., Takemura, T., and Zhang, H.: Anthropogenic and Natural Radiative Forcing, *in: Climate Change 2013: The Physical Science Basis. Contribution of Working Group I to the Fifth Assessment Report of the Intergovernmental Panel on Climate Change*, edited by: Stocker, T. F., Qin, D., Plattner, G.-K., Tignor, M., Allen, S. K., Boschung, J., Nauels, A., Xia, Y., Bex, V., and Midgley, P. M., Cambridge University Press, Cambridge, United Kingdom and New York, NY, USA, 2013.

Nakanishi, M. and Niino, H.: An improved Mellor-Yamada level-3 model with condensation physics: its design and verification, *Bound.-Lay. Meteorol.*, 112, 1–31, doi:10.1023/B:BOUN.0000020164.04146.98, 2004.

Oki, T. and Sud, Y. C.: Design of Total Runoff Integrating Pathways (TRIP) – A global river channel network, *Earth Interact.,* 2, 1–37, 1998.

Pan, H-L., and Mahrt, L.: Interaction between soil hydrology and boundary-layer development. *Bound.-Lay. Meteorol.* 38, 185-202, doi:10.1007/BF00121563, 1987.

Parker, R., Boesch, H., Cogan, A., Fraser, A., Feng, L., Palmer, P. I., Messerschmidt, J., Deutscher, N., Griffith, D. W. T., Notholt, J., Wennberg, P. O., and Wunch, D.: Methane observations from the greenhouse gases observing satellite: comparison to ground-based TCCON data and model calculations, *Geophys. Res. Lett.*, 38, L15807, doi:10.1029/2011GL047871, 2011.

Peylin, P., Law, R. M., Gurney, K. R., Chevallier, F., Jacobson, A. R., Maki, T., Niwa, Y., Patra, P. K., Peters, W., Rayner, P. J., Rödenbeck, C., van der Laan-Luijkx, I. T., and Zhang, X.: Global atmospheric carbon budget: results from an ensemble of atmospheric CO_2 inversions, *Biogeosciences*, 10, 6699-6720, doi:10.5194/bg-10-6699-2013, 2013.

Pison, I., Ringeval, B., Bousquet, P., Prigent, C., and Papa, F.: Stable atmospheric methane in the 2000s: key-role of emissions from natural wetlands, *Atmos. Chem. Phys.*, 13, 11609-11623, doi:10.5194/acp-13-11609-2013, 2013.

Prigent, C., Papa, F., Aires, F., Jimenez, C., Rossow, W. B., and Matthews, E.: Changes in land surface water dynamics since the 1990s and relation to population pressure, *Geophys. Res. Lett.*, 39, L08403, doi:10.1029/2012GL051276, 2012.

Riley, W. J., Subin, Z. M., Lawrence, D. M., Swenson, S. C., Torn, M. S., Meng, L., Mahowald, N. M., and Hess, P.: Barriers to predicting changes in global terrestrial methane fluxes: analyses using CLM4Me, a methane biogeochemistry model integrated in CESM, *Biogeosciences*, 8, 1925-1953, doi:10.5194/bg-8-1925-2011, 2011.

Saatchi, S. S., Harris, N. L., Brown, S., Lefsky, M., Mitchard, E. T., Salas, W., Zutta, B. R., Buermann, W., Lewis, S. L., Hagen, S., Petrova, S., White, L., Silman, M., and Morel, A.: Benchmark map of forest carbon stocks in tropical regions across three continents, *P. Natl. Acad. Sci.*, 108, 9899–9904, doi: 10.1073/pnas.1019576108, 2011.

Schimel, D., Stephens, B. B., and Fisher, J. B.: Effect of increasing CO2 on the terrestrial carbon cycle, *Proc. Natl. Acad. Sci.*, 112, 436–441, doi:10.1073/pnas.1407302112, 2015a.

Schimel, D., Pavlick, R., Fisher, J. B., Asner, G. P., Saatchi, S., Townsend, P., Miller, C., Frankenberg, C., Hibbard, K., and Cox, P.: Observing terrestrial ecosystems and the carbon cycle from space, *Glob. Change Biol.*, 21, 1762–1776, doi:10.1111/gcb.12822, 2015b.

Schroeder, R., McDonald, K. C., Chapman, B. D., Jensen, K., Podest, E., Tessler, Z. D., Bohn, T. J., and Zimmermann, R.: Development and Evaluation of a Multi-Year Fractional Surface Water Data Set Derived from Active/Passive Microwave Remote Sensing Data. *Remote Sensing*, 7, 16688-16732, doi:10.3390/rs71215843, 2015.

Skamarock, W. C. and Klemp, J. B.: A time-split nonhydrostatic atmospheric model for weather research and forecasting applications, *J. Comput. Phys.*, 227, 3465–3485, doi:10.1016/j.jcp.2007.01.037, 2008.

Sweeney, C., Karion, A., Wolter, S., Newberger, T., Guenther, D., Higgs, J. A., Andrews, A. E., Lang, P. M., Neff, D., Dlugokencky, E., Miller, J. B., Montzka, S. A., Miller, B. R., Masarie, K. A., Biraud, S. C., Novelli, P. C., Crotwell, M., Crotwell, A. M., Thoning, K., and Tans, P. P.: Seasonal climatology of CO_2 across North America from aircraft measurements in the NOAA/ESRL Global Greenhouse Gas Reference Network, *J. Geophys. Res. Atmos.*, 120, doi:10.1002/2014JD022591, 2015.

Turner, A. J., Jacob, D. J., Wecht, K. J., Maasakkers, J. D., Lundgren, E., Andrews, A. E., Biraud, S. C., Boesch, H., Bowman, K. W., Deutscher, N. M., Dubey, M. K., Griffith, D. W. T., Hase, F., Kuze, A., Notholt, J., Ohyama, H., Parker, R., Payne, V. H., Sussmann, R., Sweeney, C., Velazco, V. A., Warneke, T., Wennberg, P. O., and Wunch, D.: Estimating global and North American methane emissions with high spatial resolution using GOSAT satellite data, *Atmos. Chem. Phys.*, 15, 7049-7069, doi:10.5194/acp-15-7049-2015, 2015.

Uliasz, M.: Lagrangian particle modeling in mesoscale applications, *Environmental Modelling II*, ed. P. Zanetti, Computational Mechanics Publications, 71–102, 1994.

Veefkind, J. P., Aben, I., McMullan, K., Fo¨rster, H., de Vries, J., Otter, G., Claas, J., Eskes, H. J., de Haan, J. F., Kleipool, Q., van Weele, M., Hasekamp, O., Hoogeven, R., Landgraf, J., Snel, R., Tol, P., Ingmann, P., Voors, R., Kruizinga, B., Vink, R., Visser, H., and Levelt, P. F.: TROPOMI on the ESA Sentinel-5 Precursor: A GMES mission for global observations of the atmospheric composition for climate, air quality and ozone layer applications, *Remote Sens. Environ.*, 120, 70–83, doi:10.1016/j.rse.2011.09.027, 2012.

Vukicevic, T., Braswell, B. H., and Schimel, D.: A diagnostic study of temperature controls on global terrestrial carbon exchange, *Tellus, Ser. B*, 53, 150–170, doi:10.1034/j.1600-0889.2001.d01-13.x, 2001.

Wecht, K. J., Jacob, D. J., Sulprizio, M. P., Santoni, G. W., Wofsy, S. C., Parker, R., Bösch, H., and Worden, J.: Spatially resolving methane emissions in California: constraints from the CalNex aircraft campaign and from present (GOSAT, TES) and future (TROPOMI, geostationary) satellite observations, *Atmos. Chem. Phys.*, 14, 8173-8184, doi:10.5194/acp-14-8173-2014, 2014.

Whalen, S. C.: Biogeochemistry of methane exchange between natural wetlands and the atmosphere, *Environ. Eng. Sci.*, 22, 73–94, doi:10.1089/ees.2005.22.73, 2005.

Wania, R., Ross, I., and Prentice, I. C.: Implementation and evaluation of a new methane model within a dynamic global vegetation model: LPJ-WHyMe v1.3.1, *Geosci. Model Dev.*, 3, 565-584, doi:10.5194/gmd-3-565-2010, 2010.

Wilson, C., Gloor, M., Gatti, L. V., Miller, J. B., Monks, S. A., McNorton, J., Bloom, A. A., Basso, L. S., and Chipperfield, M. P.: Contribution of regional sources to atmospheric methane over the Amazon Basin in 2010 and 2011. *Global Biogeochem. Cy.*, 30, doi:10.1002/2015GB005300, 2016.

Worden, J., Kulawik, S., Frankenberg, C., Payne, V., Bowman, K., Cady-Peirara, K., Wecht, K., Lee, J.-E., and Noone, D.: Profiles of CH4, HDO, H2O, and N2O with improved lower tropospheric vertical resolution from Aura TES radiances, *Atmos. Meas. Tech.,* 5, 397-411, doi:10.5194/amt-5-397-2012, 2012.

Worden, J., Doran, G., Kulawik, S., Eldering, A., Crisp, D., Frankenberg, C., O'Dell, C., and Bowman, K.: Evaluation And Attribution Of OCO-2 XCO_2 Uncertainties, *Atmos. Meas. Tech. Discuss.*, doi:10.5194/amt-2016-175, in review, 2016.

Yokota, T., Yoshida, Y., Eguchi, N., Ota, Y., Tanaka, T., Watanabe, H., and Maksyutov, S.: Global concentrations of CO_2 and CH_4 retrieved from GOSAT: First preliminary results, SOLA, 5, 160– 163, doi:10.2151/sola.2009-041, 2009.

Tables

Table 1: Observation system characteristics[a]

Observation System	Single sounding footprint size	Single CH_4 measurement precision	Visits per day
LEO	7km × 7km	0.6% (10.8 ppb)	1
GEO	3km × 3km	0.6% (10.8 ppb)	4
LEO+[b]	7km × 7km	0.42% (7.6 ppb)	1
GEO×2	3km × 3km	0.6% (10.8 ppb)	8
GEO-Z1	3km × 3km	0.6% (10.8 ppb)	4[c]
GEO-Z2	3km × 3km	0.6% (10.8 ppb)	4[d]

[a]LEO and GEO observation parameters are broadly consistent with TROPOMI and GEOCAPE simulations by Wecht et al.,(2014); to simplify comparisons, we set GEO and LEO default single CH_4 sounding precision to 0.6%.

[b]Single measurement precision is a factor of $\sqrt{2}$ higher than LEO; this is the equivalent to doubling the visits per day for LEO.

[c]2 (6) visits per day in 0 – 50%ile (50 – 100%ile) cloud-cover areas;

[d]2 (10) visits per day in 0 – 75%ile (75 – 100%ile) cloud-cover areas;

Figures

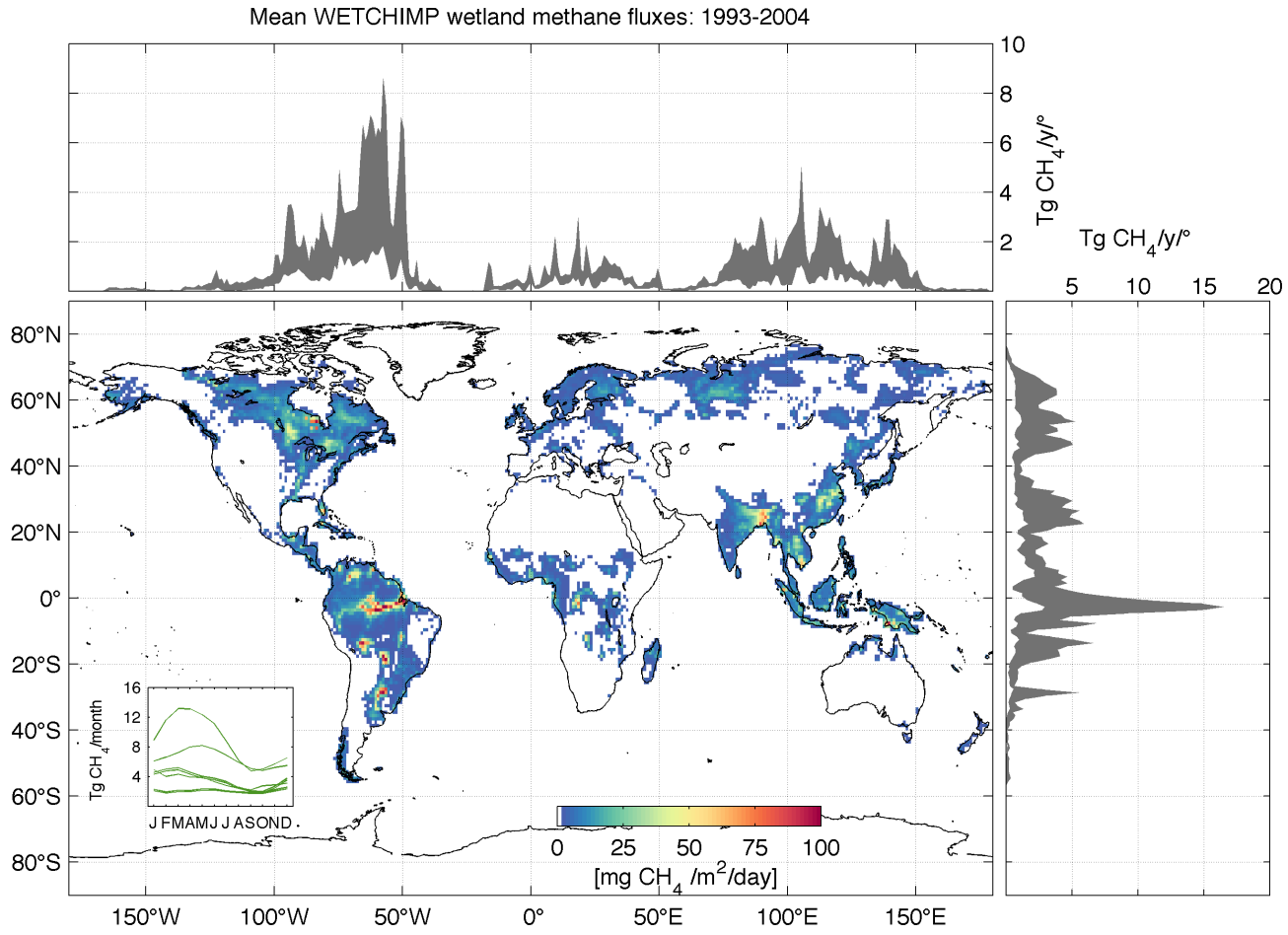

Figure 1: Mean annual wetland and rice CH_4 emissions (central maps), and associated longitudinal and latitudinal uncertainty (grey bands), based on the WETCHIMP model inter-comparison project (Melton et al., 2013). **Inset**: WETCHIMP model total Amazon basin monthly CH_4 emissions.

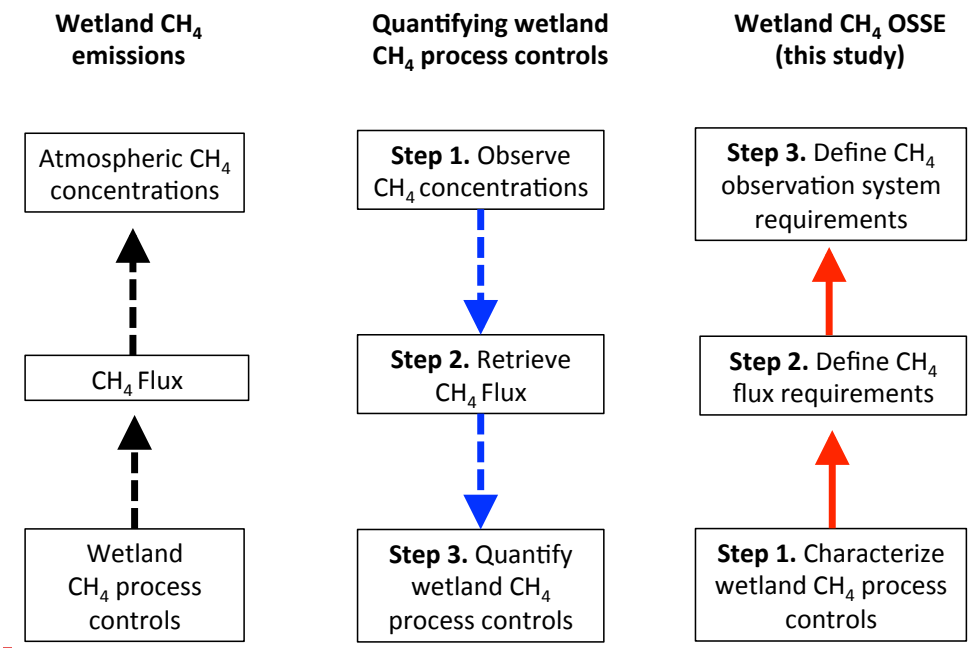

Figure 2. Wetland CH_4 emissions into the atmosphere are regulated by wetland biogeochemical processes (left column). Continental-scale wetland CH_4 process controls can be retrieved by (i) resolving surface CH_4 fluxes from retrieved satellite CH_4 observations; (ii) resolving process parameters from retrieved CH_4 fluxes (middle column). The optimal satellite CH_4 observation requirements are a function of the flux resolution and precision required to resolve wetland CH_4 process controls (right column): OSSE steps 1-3 are described in sections 2.1-2.3.

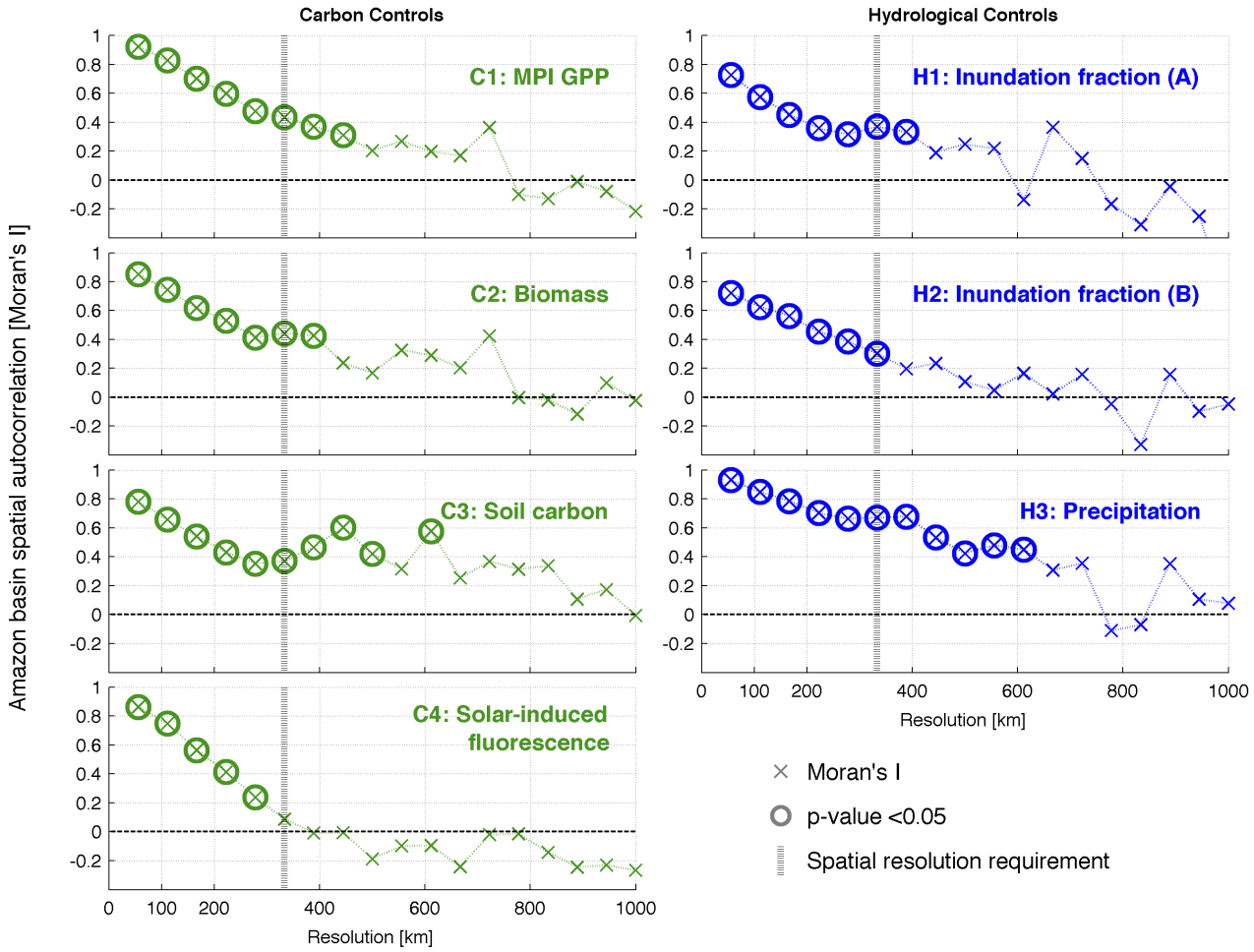

Figure 3: Spatial autocorrelation (Moran's I) for potential carbon controls (left column) and hydrological controls (right column) on wetland CH_4 emissions. The spatial variability of carbon controls are derived from satellite observations (Biomass, Saatchi et al., 2011; solar induced fluorescence; Joiner et al., 2013), the Harmonized World Soil database (soil carbon, Hiederer & Köchy, 2011) and FLUXNET derived GPP (Jung et al., 2009). The spatial variability estimates for hydrological controls are based on satellite measurements of inundation (A: Prigent et al., 2007; B: Schroeder et al., 2015), and precipitation (the NASA Tropical Rainfall Measuring Mission). Significant Moran's I values (where the Moran's I p-value < 0.05) are highlighted as circles. We set a ~333km spatial resolution requirement for monthly CH_4 flux retrievals,

based on the maximum correlation lengths of potential carbon and hydrological controls on wetland CH_4 emissions. The details of the Moran's I analysis are fully described in Appendix A.

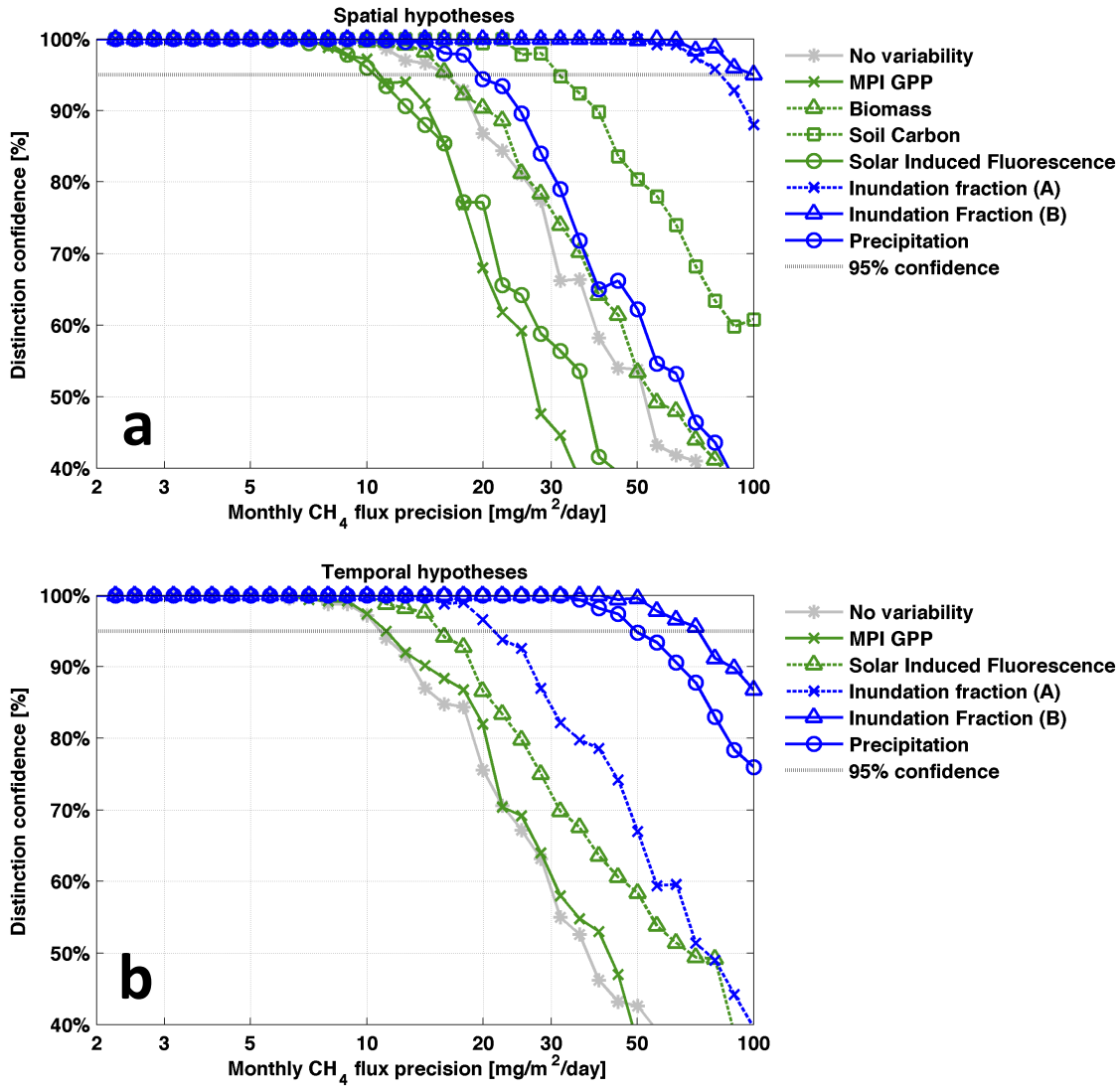

Figure 4: Distinction confidence between Amazon basin spatial and temporal wetland CH_4 emission hypotheses against monthly ~333km x 333km CH_4 flux precision. Spatial and temporal wetland CH_4 emission hypotheses are distinguishable

with a 95% confidence at a <10 mg m^{-2} day^{-1} precision. For this study we define our ~333km x 333km CH_4 flux precision requirement as 10 mg m^{-2} day^{-1}.

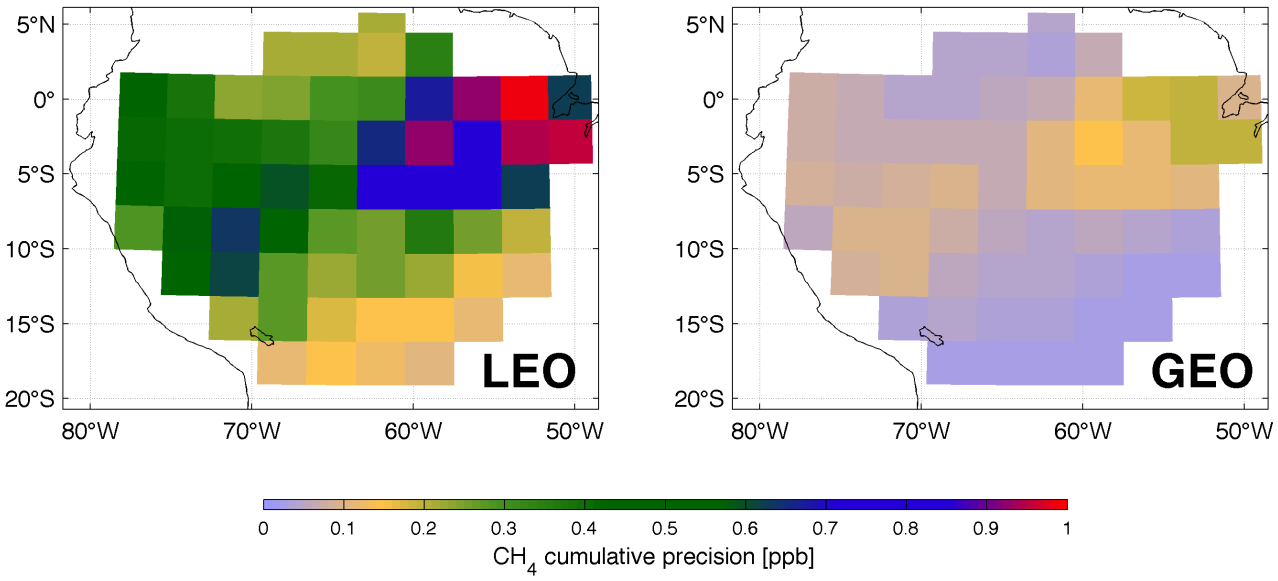

Figure 5: Retrieved monthly ~333km CH_4 cumulative precision (i.e. the combined precision of monthly-averaged CH_4 measurements) for LEO and GEO observing systems (OS); the OS configurations are described in Table 1.

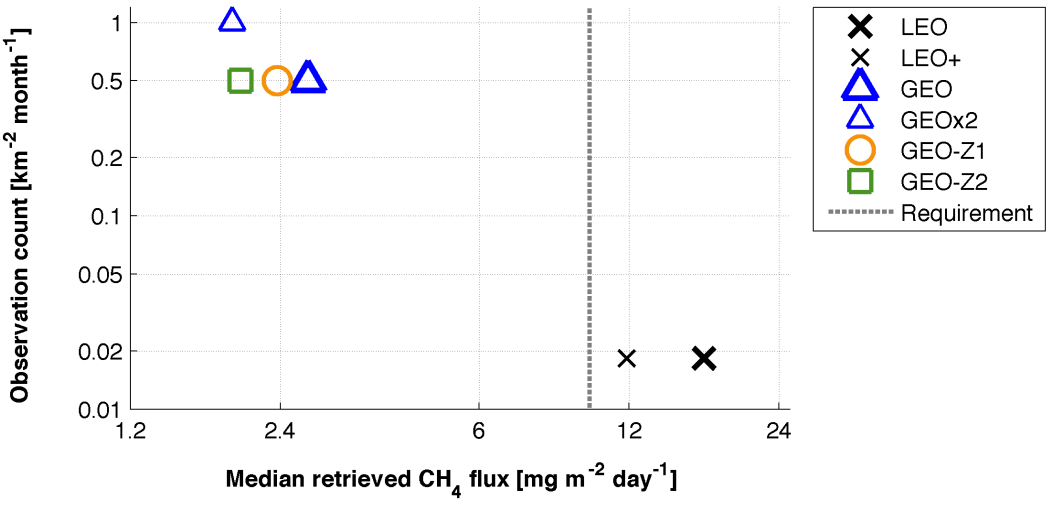

Figure 6: CH_4 observations density (observations per unit area; y-axis) versus retrievable ~333km flux precision (x-axis) for six CH_4 observation systems (see Table 1 for details). The "observation density" includes all attempted CH_4 measurements, including accepted (cloud-free) and rejected (cloudy) observations.

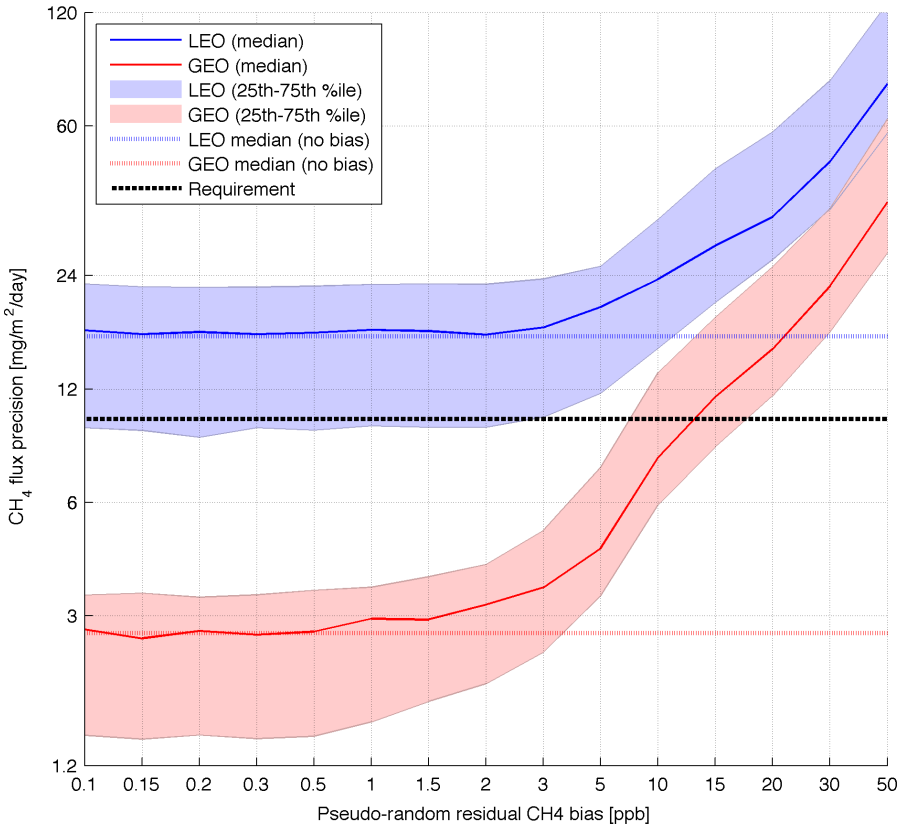

Figure 7: Retrieved GEO and LEO flux precision for L = ~333km with modelled pseudo-random residual bias error. See table 1 for details on GEO and LEO CH_4 observing systems.

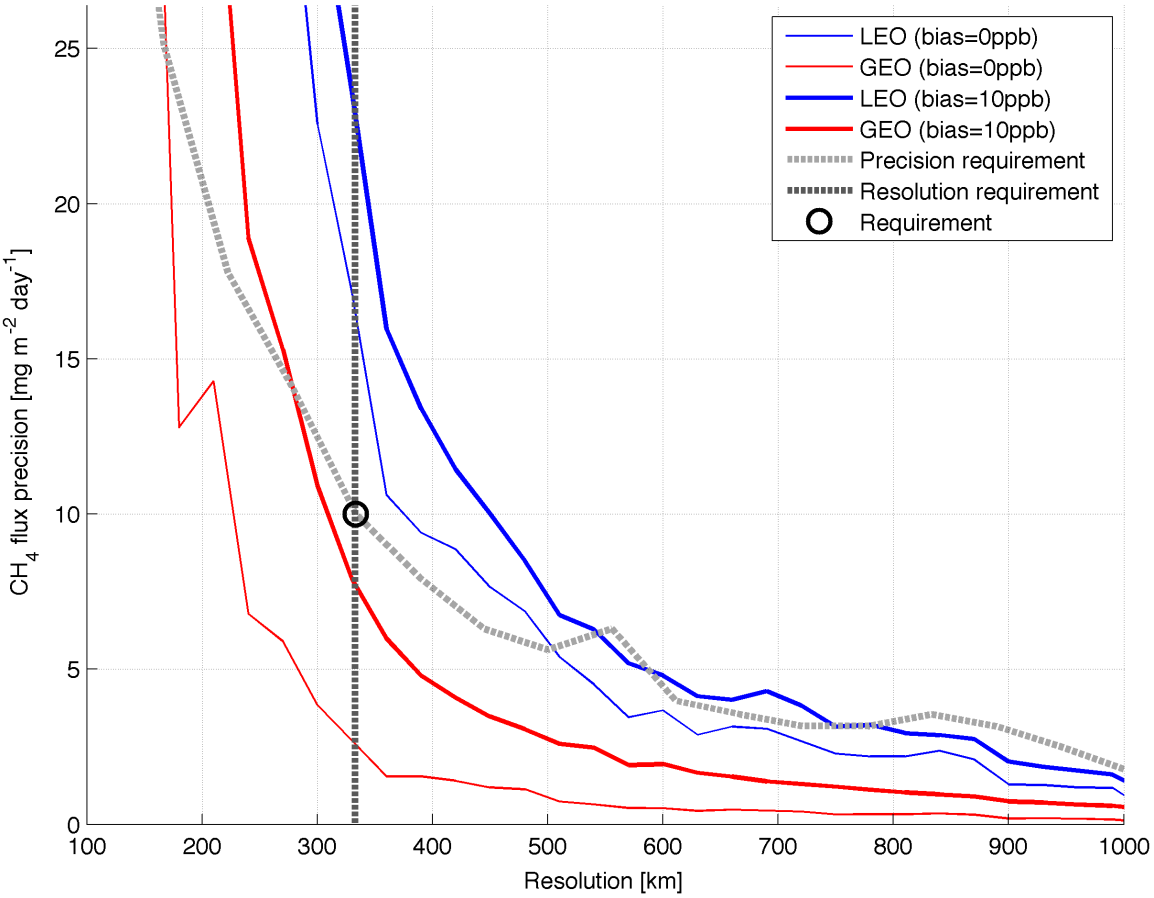

Figure 8: Median retrieved LEO and GEO CH_4 fluxes for L = 150 – 990km; the dashed lines indicate precision and resolution requirements. See table 1 for details on GEO and LEO CH_4 observing systems. The bias value of 10ppb indicates modelled systematic CH_4 measurement biases with 100km spatial correlations (see section 2.3).

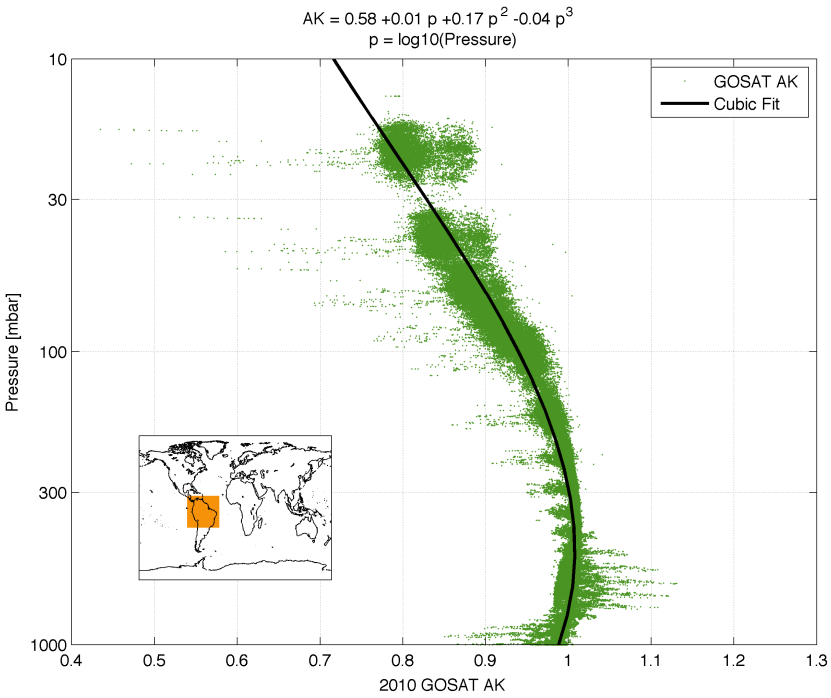
AK = 0.58 +0.01 p +0.17 p^2 -0.04 p^3
p = log10(Pressure)
GOSAT AK
Cubic Fit
Pressure [mbar]
10
30
100
300
1000
0.4
0.5
0.6
0.7
0.8
0.9
1
1.1
1.2
1.3
2010 GOSAT AK

Figure A1. January to December 2010 GOSAT averaging kernels (AK) for the broader Amazon region (green dots). The black line denotes the AK cubic fit (w.r.t. pressure *p*; equation shown at the top of the figure). This AK was used to vertically weight the LPDM footprint and sample WRF CH_4 concentrations (see Appendix D).

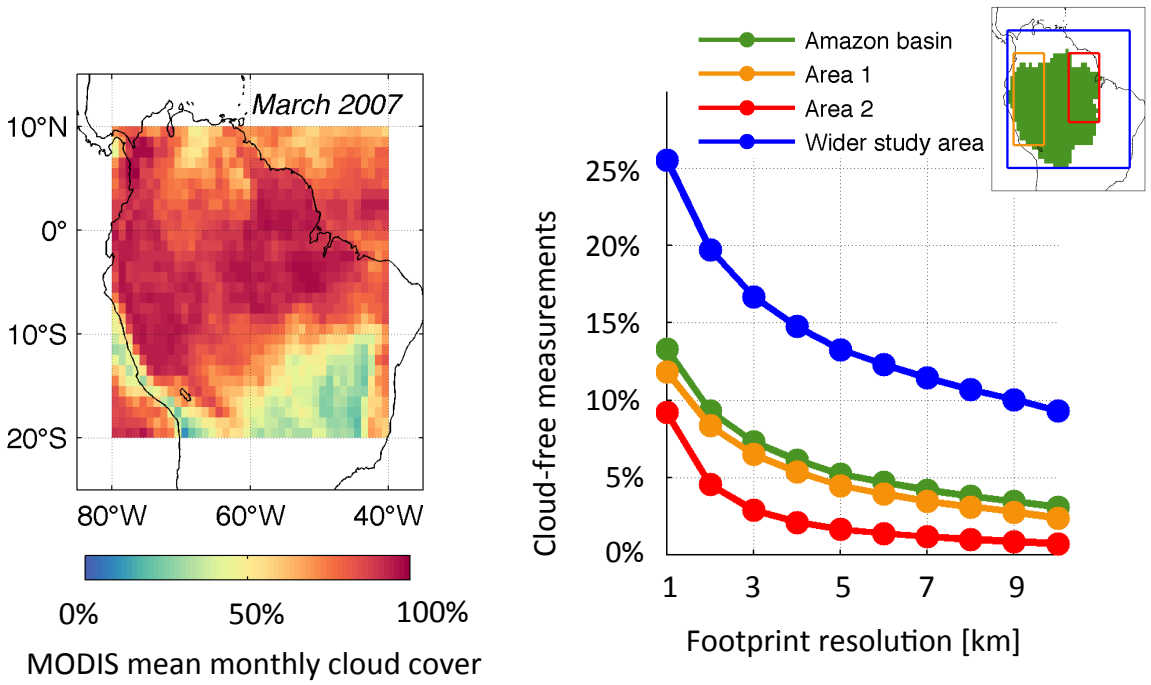

Figure B1. **Left:** March 2007 mean MODIS cloud cover aggregated to 1° ×1°. **Right:** Summary of March 2007 cloud-free observations versus footprint size for the broader study area, the Amazon river basin, and two sub-regions (east and west Amazon river basin).

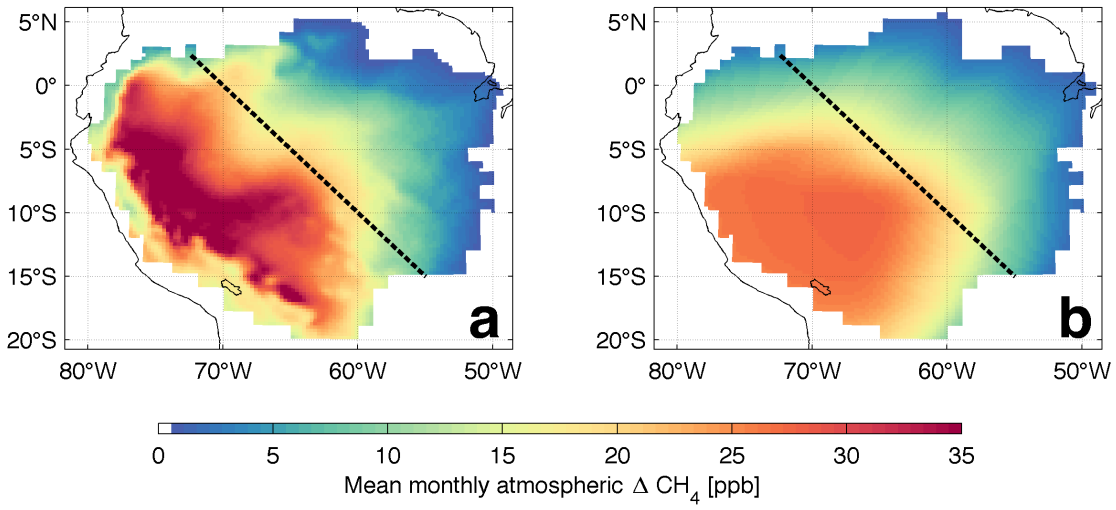

Figure D1. March 2007 simulations of atmospheric CH_4 concentration enhancements – based on 12 mg m^{-2} day^{-1} fluxes throughout the Amazon basin – derived using the WRF atmospheric transport model (**a**) and the LPDM influence function approach (**b**). The dashed line denotes our delineation of "North-East Amazon basin" and "South-West Amazon basin" regions (see Appendix C).